The head of the earwig *Forficula auricularia* (Dermaptera) and its evolutionary implications

DAVID NEUBERT[1], SABRINA SIMON[2], ROLF G. BEUTEL[1] & BENJAMIN WIPFLER *, [1]

[1] Institut für Spezielle Zoologie und Evolutionsbiologie, FSU Jena, 07743 Jena, Erbertstraße 1, Germany; Benjamin Wipfler * [benjamin.wipfler @uni-jena.de] — [2] Biosystematics Group, Wageningen University, Wageningen, The Netherlands — * Corresponding author

Abstract

The external and internal head morphology including the musculature of the common earwig *Forficula auricularia* is described in detail. We specified and corrected previous descriptions and provided a detailed documentation. The head of *Forficula* is characterized by prognathism, generalized mandibles with a mesal cutting edge distally of the mola and its drop-shaped appearance. We added the following new apomorphies for Dermaptera to the various previously reported ones: (I) coronal and frontal cleavage lines with corresponding strong internal strengthening ridges; (II) the division of the praementum into a basal and a distal sclerite; (III) the presence of a bumpulus at the tip of the paraglossa; (IV) the presence of large distal palpilla on the terminal maxillary and labial palpomeres and (V) the origin of M. tentoriohypopharyngealis on the submentum. Another potential apomorphy are the lateral lobes on the distal hypopharynx which are most likely not homologous to the superlingua of apterygote insect. Other characters such as the prominent ball-and-socket joint between scapus and pedicellus or the unique antennal heart are poorly studied within Dermaptera and therefore cannot be phylogenetically polarized. In contrast to the various ordinarial apomorphies, the dermapteran head exhibits only one potential synapomorphy with other polyneopteran orders: the absence of the linguactual tendon and the associated muscle that is shared with Plecoptera and/or Zoraptera. Our results show that additional studies of the presumingly basal splits of Dermaptera are required to understand the head evolution of the group.

Key words

1.   Introduction

With about 2000 (ZHANG 2011) described species, Dermaptera is one of the smaller insect orders. Despite this relatively low species number, earwigs are widely known insects. This is partly due to their distinctive and largely uniform habitus, with large pincer-shaped cerci, shortened sclerotized forewings and an elongate flattened body. Another reason is the widespread believe that they infest human ears, where they deposit their eggs or even penetrate into the brain. This is reflected in their common names as for instance earwig in English, perce-oreille ("ear-piercer") in French, "Ohrwurm" ("ear-worm") in German, or ukhovertka ("ear-turner") in Russian. The source of this superstition is most likely the Latin author Pliny the Elder who lived in the first century A.D. (BERENBAUM 2007). However, there is only one badly documented case where an earwig indeed infested a human acoustic meatus (BERENBAUM 2007). This stands in clear contrast to other insects, especially roaches, beetles and honeybees that have a well-documented record of entering human ears (BRESSLER & SHELTON 1993; ANTONELLI et al. 2001; RYAN et al. 2006).

Despite their general publicity, the group received comparatively little attention from scientists. Few researchers deal with the order and the bulk of information

Table 1. Proposed sistergroups for Dermaptera with literature and data source.

Proposed sistergroup	Literature source	Source of data
Plecoptera	KJER 2004	18S
	YOSHIZAWA & JOHNSON 2005	18S
	KJER et al. 2006	18S
	MISOF et al. 2007	18S
	SIMON et al. 2010	EF-1α
	ISHIWATA et al. 2011	DPD1, RPB1, RPB2
	WIPFLER et al. 2011	head morphology: cladistic analysis
	DJERNAES et al. 2012	COI, COII, 16S, 18S, 28S
	WAN et al. 2012	mitochondrial genome
	YOSHIZAWA 2011	wing joint morphology: cladistic analysis
	FRIEDEMANN et al. 2012	head morphology: cladistic analysis
	SIMON et al. 2012	transcriptomic data
	LETSCH & SIMON 2013	transcriptomic data
	WANG et al. 2013	18S rDNA
	MA et al. 2014	mitochondrial genome
	SASAKI et al. 2014	DPD1, RPB1, RPB2
	YU-HAN et al. 2014	mitochondrial genome
	WU et al. 2014	mitochondrial genome
	NAEGLE et al. 2016	18S, 28S, COI, Histone 3, TUBA
	SONG et al. 2016	mitochondrial genome
Dictyoptera	HENNIG 1969	morphology: discussion
	HAAS & KUKALOVÁ-PECK 2001	wing morphology: discussion
Grylloblattodea	KAMP 1973	morphology: numerical analysis
Xenonomia	YOSHIZAWA 2011	morphology: cladistic analysis
Eukinolabia	BLANKE et al. 2012	head morphology: cladistic analysis
Embioptera	BLANKE et al. 2013	head morphology: cladistic analysis
Orthoptera	KOMOTO et al. 2012	mitochondrial genome
	ZHOU et al. 2016	mitochondrial genome
Zoraptera	TERRY & WHITING 2005	18S rDNA, 28S rDNA, Histone 3 & morphology
	JARVIS et al. 2005	18S rDNA, 28S rDNA, Histone 3 & morphology
	MISOF et al. 2014	transcriptomic data
Phasmatodea	BLACKITH & BLACKITH 1967	morphology: discussion
(Orthoptera + Phasmatodea) + Xenonomia	GRIMALDI & ENGEL 2005	morphology: discussion
((Phasmatodea + Orthoptera) + Dictyoptera) + Xenonomia	BEUTEL & GORB 2006	morphology: cladistic analysis
Caelifera + (Plecoptera + Xenonomia)	WIPFLER 2012	head morphology: cladistic analysis
(Embioptera + Zoraptera + Xenonomia) + Phasmatodea + Orthoptera + Dictyoptera	WIPFLER et al. 2015	thorax morphology: cladistic analysis

presently available is restrained to the "common" species *Forficula auricularia*, *Anisolabis maritima* or *Labidura riparia*.

One of the major challenges is the evolutionary origin of the group. It is well established that the order Dermaptera is part of the lower neopteran insects or Polyneoptera. However, this lineage is problematic with respect to its monophyly and interordinal relationships (see BEUTEL et al. 2014a for a review). Virtually every other polyneopteran group was proposed as sistergroup of Dermaptera (Table 1). The currently best-supported hypotheses are a clade Dermaptera + Plecoptera which is supported by various independent character systems (Table 1) and two transcriptomic studies (SIMON et al. 2012 and LETSCH & SIMON 2013) or Zoraptera + Dermaptera suggested recently by a comprehensive transcriptomic analysis including 1478 genes and 144 species representing all traditional orders (MISOF et al. 2014). However, both hypotheses lack convincing morphological arguments and all transcriptomic studies so far show

uncertainties of unstable positions. A complex data set of cephalic characters that was analyzed in several studies with an increasing taxon sampling (WIPFLER et al. 2011; FRIEDEMANN et al. 2012; BLANKE et al. 2012, 2013; WIPFLER 2012; MATSUMURA et al. 2015) provided highly ambiguous results for the placement of Dermaptera (Table 1). Cladistic analysis of characters of the wing joint (YOSHIZAWA 2011) and thorax (WIPFLER et al. 2015) resulted in two new hypotheses not proposed in any studies based on characters of the head. A part of the consistent problem is a surprising lack of detailed morphological data, also concerning the head morphology. Studies on cephalic structures were presented for the following earwigs: *Anisolabis maritima* (Anisolabididae) (YUASA 1920; DORSEY 1943; WALLER et al. 1996), *Forficula auricularia* (KÜHNLE 1913; WALKER 1931, 1933; STRENGER 1950; HENSON 1950; POPHAM 1959; MOULIN 1969; PASS 1988; WALLER et al. 1996), *Labidura riparia* (Labiduridae) (KADAM 1961; GILES 1962; KHANDEKAR 1972, 1973; WALLER et al. 1996), *Anisolabis littorea* (Anisolabididae),

Echinosoma afrum (Pygidicranidae), *Bormansia africana* (Pygidicranidae), *Chaetospania brunneri* (Spongiphoridae), *Chelisoches morio* (Chelisochidae) (Giles 1962), *Arixenia esau* (Jordan 1909), *Arixenia jacobsoni* (Arixenidae) (Giles 1961, 1962; Waller et al. 1996), *Hemimerus esau*, *Hemimerus hanseni* (Giles 1962) and *Hemimerus talpoides* (Hemimeridae) (Hansen 1894; Jordan 1909; Giles 1961; Waller et al. 1996). Despite this impressive list, not a single complete description of the cephalic skeleto-muscular system of any earwig species is presently available. Additionally, several previous studies contradict each other. This induced us to re-evaluate the head morphology of the well-known *Forficula auricularia*, with a strong focus on a detailed morphological documentation, using a broad spectrum of current morphological techniques. Since Popham (1959) already provided a discussion of the mouthpart function of this species, we will focus our study on the evolutionary and phylogenetic implications of the morphological findings.

2. Material & methods

Specimens of *Forficula auricularia* Linnaeus, 1758 (Dermaptera, Forficulidae) were collected in Weimar, Thuringia, Germany by DN (summer 2014) and preserved in 70% ethanol.

Samples were transferred in 100% acetone and critical point dried with an Emitech K850 critical point dryer (Quorum Technologies, East Grunstead, England). For digital microscopy, the dried samples were mounted on a special sample holder (Pohl 2010) and photographed with a Keyence VHX 2000 (Keyence Deutschland GmbH, Neu-Isenburg, Germany). One female specimen was used for μ-computed tomography. The scan was performed at BESSY2 of the Berliner Elektronenspeicherring-Gesellschaft für Synchrotronstrahlung (Berlin, Germany; resolution: 2.486 μm; exposure time: 400 ms; 1000 projections with an angle of 0.18°). The data set is stored in the collection of the Phyletisches Museum, Jena, Germany. Additionally the CT-scan can be downloaded from Morphobank (http://www.morphobank.org; project 2531). We used Amira 5.3.1 (Visage Imaging GmbH, Berlin, Germany) to segment the different materials. Subsequently we exported every individual material as tiff image stack into VGStudio Max 2.0.5 (Volume Graphics GmbH, Heidelberg, Germany) for volume rendering. For scanning electron microscopy, samples were sputter coated with an Emitech K500. Microscopy was performed with a Philips XL30 ESEM (Philips Deutschland, Hamburg, Germany) with a rotatable sample holder (Pohl 2010).

The illustrations are based on 3D reconstructions and were drawn with Adobe Illustrator CS6 (Adobe, San Jose, California, USA). All images and plates were edited with Adobe Photoshop CS6 and Adobe Illustrator CS6 (Adobe, San Jose, California, USA).

The general morphological terminology follows Beutel et al. (2014b). The terms for the hypopharynx are taken from Buder & Klass (2013). The muscles are labeled in consecutive numbers according to their appearance. In the discussion, we present a homologisation with the terminology of Wipfler et al. (2011).

We distinguish between formative elements or structure such as the labrum or the galea (abbreviated in small letters) and sclerites which are located on these structures such as the labral sclerite (abbreviated in capital letters) as proposed by Wipfler et al. (2016). We also follow Wipfler et al. (2016) by distinguishing between ridges (strengthening lines on a sclerite), syndeses (membranous connections between two sclerites) and ecdysial cleavage lines.

3. Results

3.1. Head capsule
Figs. 1, 2, 3

The head is prognathous and dorso-ventrally flattened (Figs. 1, 2). Its color is brownish (Fig. 1) and it is strongly sclerotized. In dorsal view it is approximately drop-shaped with its broadest point either at the level of the compound eyes or behind them, and narrowing anteriorly. It is slightly longer than broad. The height of the head capsule is approximately half of the maximum length. The surface is sparsely covered with setae, more densely on the posterior half.

The foramen occipitale (foc, Fig. 3) is nearly rectangular, with a rounded dorsal margin and slightly narrowed at its ventral edge. It is surrounded by the postocciptal ridge. The gula (g, Figs. 1, 2, 13) is adjacent antero-ventrally. It is nearly rectangular, approximately 4 times as long as broad. Its posterior border to the foramen occipitale is slightly concave. Thin ridges (gr, Fig. 2) enclose the gula laterally. The broad coronal cleavage line originates dorso-medially from the foramen occipitale (co, Figs. 1, 2) and continues in the midline along the dorsal side of the head capsule, thus dividing the vertex. Slightly posteriorly the compound eyes it branches into 2 diverging frontal cleavage lines (fs, Figs. 1, 2, 13) which continue laterally and end at the mesal edge of the compound eyes, at the point of the smallest distance between them. Externally the frontal and the anterior part of the coronal cleavage line is visible as depressed lines. Posteriorly it widens strongly. Internally the coronal and frontal cleavage lines are supported by ridges. The laterally placed oval compound eyes (ce, Figs. 1, 2, 3, 4) are twice as high as long. They are enclosed by the circumocular ridge (cor, Fig. 1). Ocelli are absent. The attachment sites of dorsal tentorial arms (dtap, Figs. 1, 2) are very distinct on the dorsal surface of the head capsule, slightly mesad the compound eyes and anterior to the frontal cleavage lines. The antennal sockets anterior to the compound
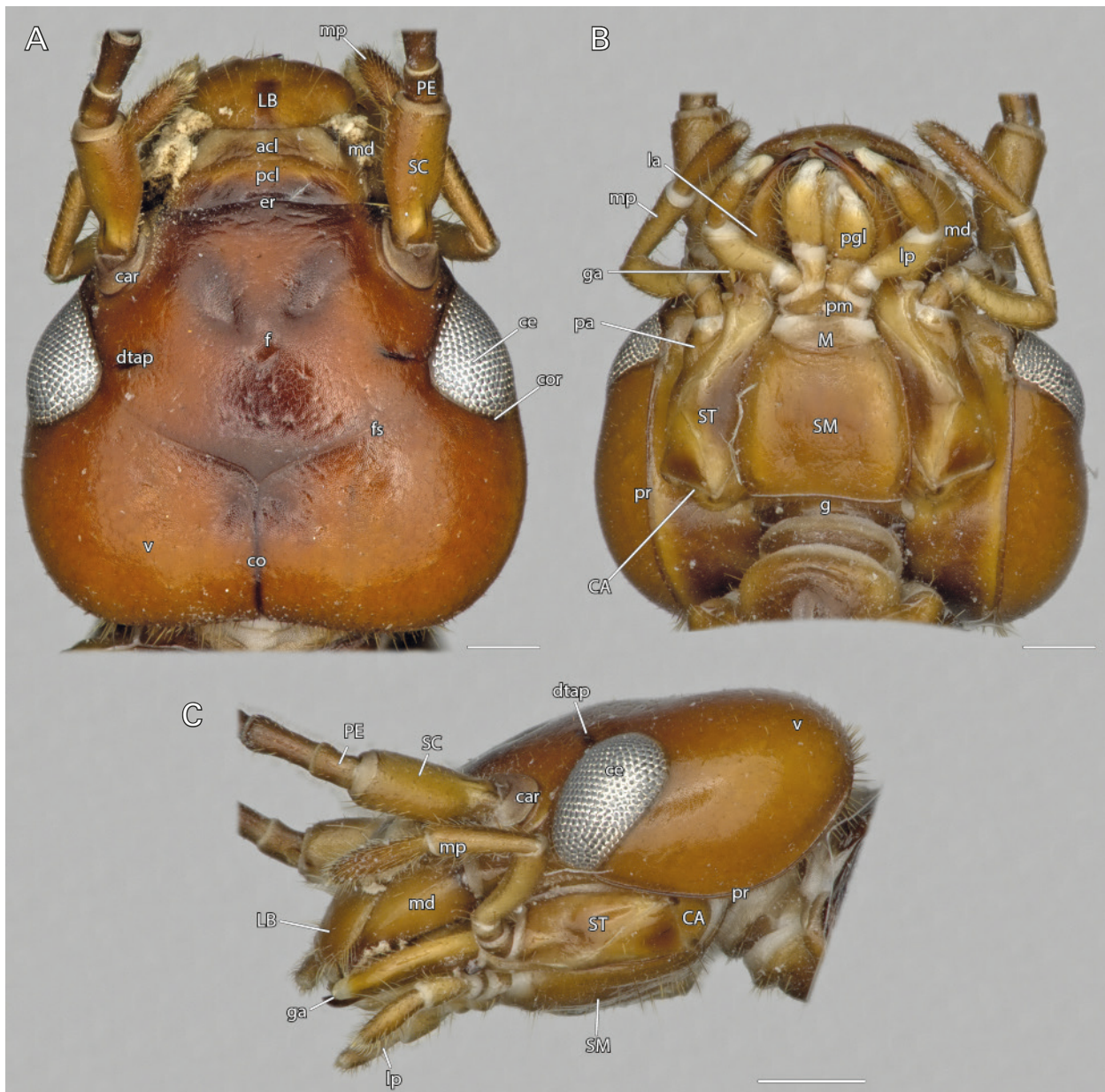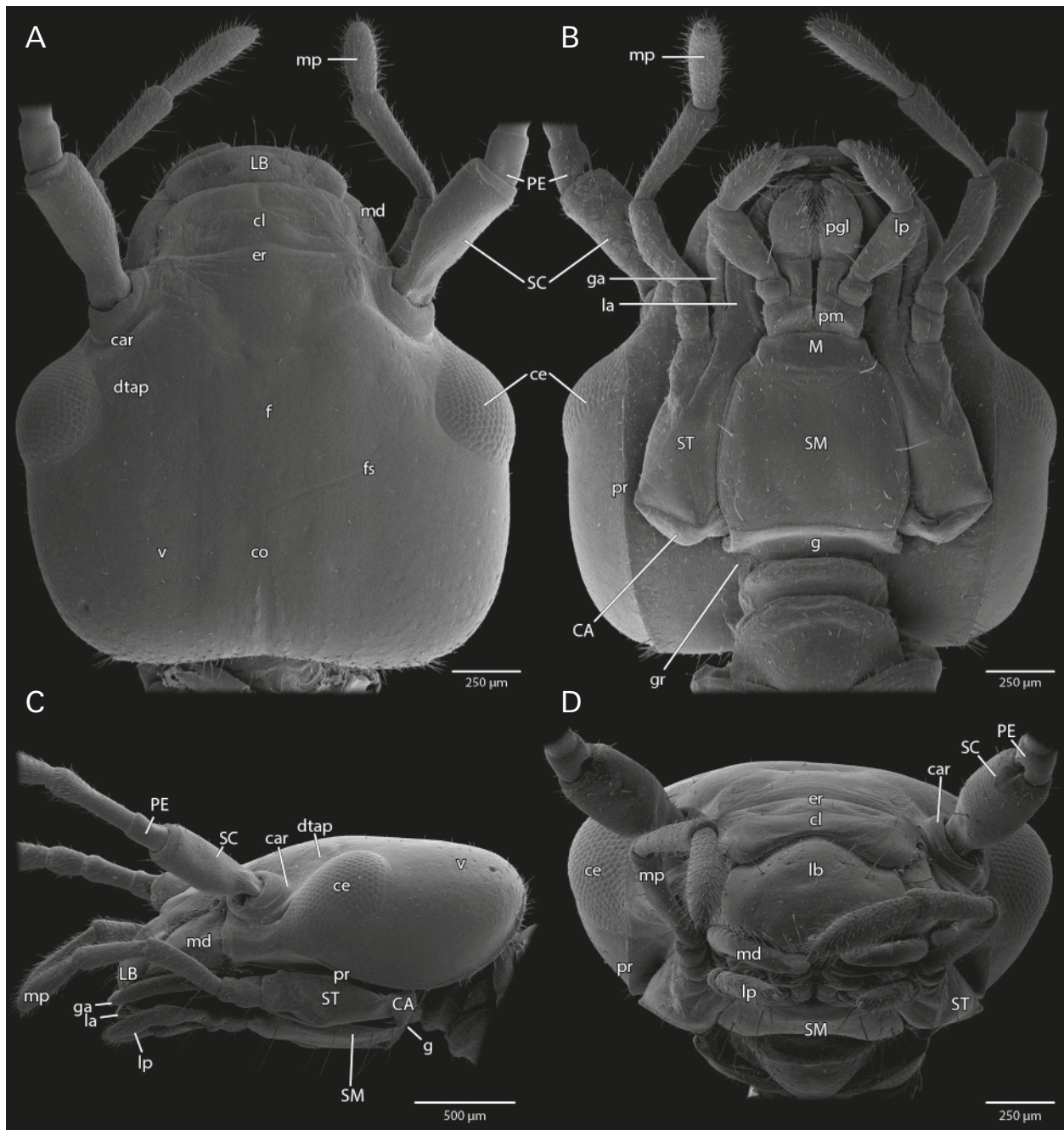
Fig. 1. *Forficula auricularia*, head, digital photography. **A**: dorsal view; **B**: ventral view; **C**: lateral view. — ***Abbreviations***: acl – anteclypeus; CA – cardinal sclerite; car – circumantennal ridge; ce – compound eyes; co – coronal cleavage line; cor – circumoccular ridge; dtap – dorsal tentorial pit; er – epistomal ridge; f – frons; fs – frontal cleavage line; g – gula; ga – galea; la – lacinia; LB – labral sclerite; lp – labial palpus; M – mental sclerite; lp – labial palpus; M – mental sclerite; md – mandible; mp – maxillary palpus; pa – palpifer; pcl – postclypeus; PE – pedicellus; pgl – paraglossa; PM – praemental sclerite; pr – parietal ridge; SC – scapus; SM – submental sclerite; ST – stipital sclerite; v – vertex. — Scale bar: 500 μm.

eyes are surrounded by circumantennal ridges (car, Figs. 1, 2, 4), which bear a ventro-lateral process, the antennifer (ant, Fig. 4).

The well-developed epistomal ridge (er, Figs. 1, 2, 13) connects the two anterior mandibular articulations. It separates the basal clypeal region from the frons (f, Figs. 1, 2). The clypeus (cl, Figs. 2, 3) is trapezoid and narrowing distally. It is composed of a proximal sclerotized postclypeus (pcl, Fig. 1) and a distal semimembranous anteclypeus (acl, Fig. 1). The postclypeus bears several long setae. Distally the edge of the clypeus lies slightly

above the labrum. Both structures are connected by a syndesis that allows movements of the labrum.

The pleurostomal ridge is the lateral continuation of the epistomal one. It is strongly curved and in its dorsal half it continues from the anterior mandibular articulation postero-ventrad until it reaches the circumocular ridge. In this area it is connects with the circumantennal ridge and supports the anterior tentorial pit (atap, Fig. 4), which is externally visible as a depression. The second section of the pleurostomal ridge extends from the circumocular ridge towards the posterior mandibular joint.

Fig. 2. *Forficula auricularia*, head, scanning electron micrograph. **A**: dorsal view; **B**: ventral view; **C**: lateral view; **D**: frontal view. — ***Abbreviations***: CA – cardinal sclerite; car – circumantennal ridge; ce – compound eyes; cl – clypeus; co – coronal cleavage line; dtap – dorsal tentorial pit; er – epistomal ridge; f – frons; fs – frontal cleavage line; g – gula; ga – galea; gr: gular ridge; la – lacinia; LB – labral sclerite; lp – labial palpus; M – mental sclerite; md – mandible; PE – pedicellus; pgl – paraglossa; PM – praemental sclerite; pr – parietal ridge; SC – scapus; SM – submental sclerite; ST – stipital sclerite; v – vertex.

The hypostomal ridge continues at this articulation and forms the maxillary fossa and labial insertion area. It ends at the posterior tentorial pits formed at the junction of the postoccipital ridge and posterior tentorial arms. The strong parietal ridge (pr, Figs. 1, 2) is the posterior continuation of the ventral half of the pleurostomal and the ventral circumoccular ridge. It runs posteriorly from the postero-ventral edge of the circumoccular ridge along the lateral sides of the head capsule. It obliterates in the posteriormost cephalic region.

3.2. Tentorium
Fig. 3

The tentorium is well developed and comprises the corpotentorium (ct, Figs. 3, 13, 14) and the posterior (pta, Figs. 3, 13), anterior (ata, Figs. 3, 13) and dorsal tentorial arms (dta, Figs. 3, 13). The short and massive posterior arms originate at the posterior tentorial pits at the junction of the postoccipital ridge and the hypostomal ridge. The long plate-like corpotentorium is anteriorly about twice
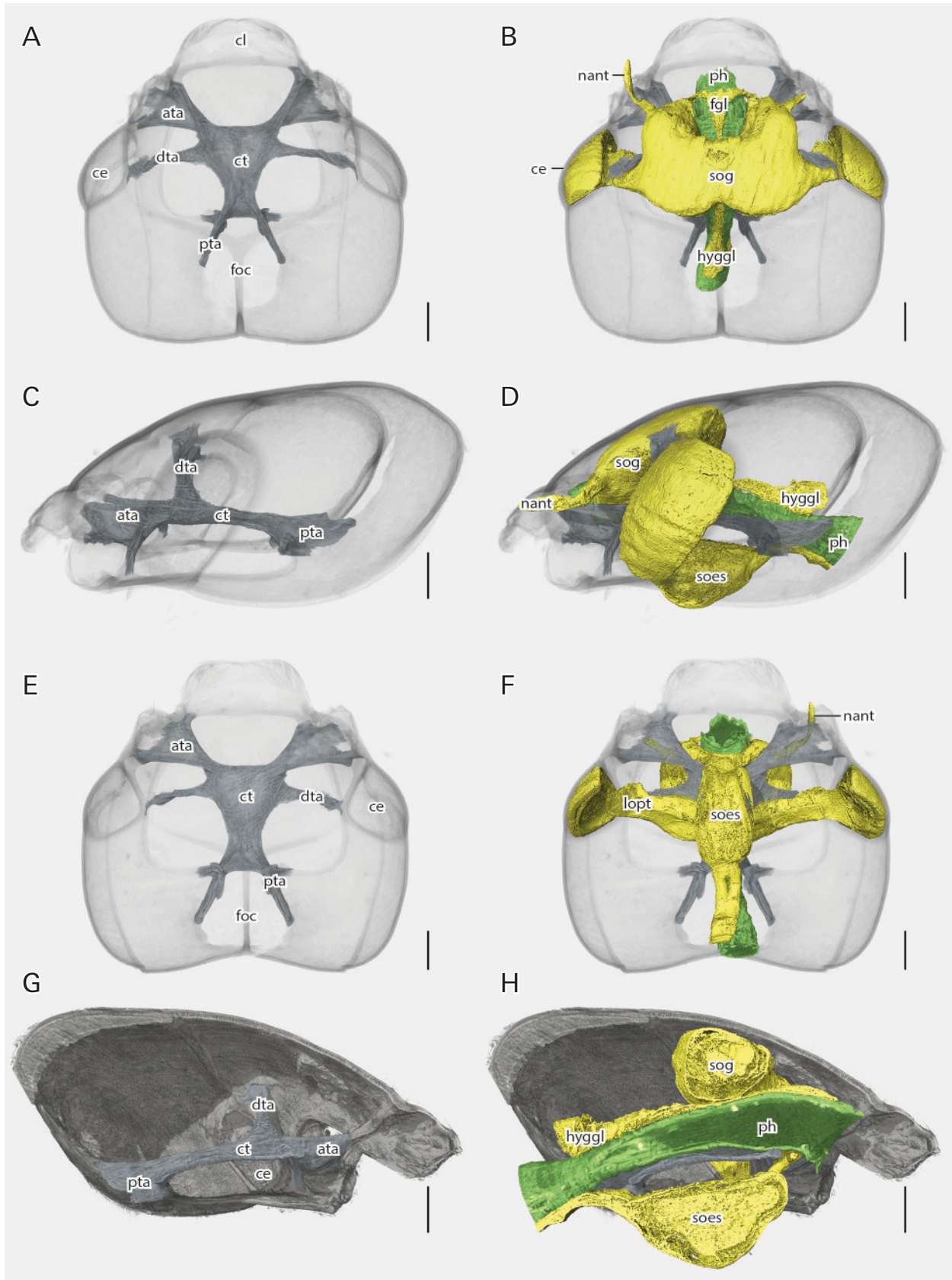
Fig. 3. *Forficula auricularia*, head capsule, endoskeleton, 3d-reconstruction. **A**: dorsal view; **B**: dorsal view, nervous and digestive system; **C**: lateral view; **D**: lateral view, nervous and digestive system; **E**: ventral view; **F**: ventral view, nervous and digestive system; **G**: midsagittal view; **H**: midsagittal view, nervous and digestive system. — ***Abbreviations***: ata – anterior tentorial arm; ce – compound eyes; cl – clypeus; ct – corpotentorium; dta – dorsal tentorial arm; fgl – frontal ganglion; foc – foramen occipitale; hyggl – hypocerebral ganglion; lopt – lobus opticus; nant – nervus antennalis; ph – pharynx; pta – posterior tentorial arm; soes – suboesophageal ganglion; sog – supraoesophageal ganglion. — Scale bar: 200 μm.

as wide as in its posterior third. The massive dorsal and anterior arms arise from its anterior third. The dorsal arms arise from the dorsal surface of the corpotentorium and continue dorso-laterally where they attach to distinct internal convexities of the head capsule. The anterior arms arise from the antero-lateral corpotentorial edges. They are twisted about 180°, the left clockwise and the right one counterclockwise. Anteriorly they widen strongly, resulting in a triangular shape. They connect with the anterior tentorial pits on the pleurostomal ridge.

3.3. Antennae
Fig. 4

The antennae are long and slender, approximately 2.5 – 3 times as long as the head capsule and approximately half as long as the body without cerci. They are brownish but less pigmented than the remaining head capsule. They are composed of scapus (SC, Figs. 1, 2, 4, 13), pedicellus (PE, Figs. 1, 2, 4) and a flagellum with twelve flagellomeres. However, in several studied specimens the distal flagellomeres apparently broke off and a scar-like wound closure is present (Fig. 4E,F). The scapus is twice as long as wide and sparsely covered with setae. A ventral cavity at the base articulates with the antennifer. The pedicellus is as long as the diameter of the scapus and only slightly longer than wide. It is sparsely covered with setae. Mesally on its distal part, the scapus forms an infolded protrusion which articulates with a large depression on the pedicellus, thus forming a joint similar to the antennifer-scapus articulation. The club-shaped first flagellomere is three times as long as wide at its base and extended distally. The density of the setation increases distally. Flagellomere two is the shortest, with only half the length of the basal one. Like all following segments it is densely covered with setae. Flagellomeres three – twelve are similar in appearance and approximately twice as long as wide. Flagellomere twelve is distally rounded and holds several setae.

3.4. Labrum & epipharynx
Figs. 1, 2, 5

The rhomboid labrum is rounded at its anterior margin. A narrow membranous syndesis connects its proximal edge with the anterior clypeal margin. Four pairs of long setae and several short ones are inserted on the surface. The anterior labral region is sclerotized (LB, Figs. 1, 2, 13). The inner wall of the labrum is formed by membranous anterior epipharynx (epi, Figs. 13). The short and sclerotized tormae (TO, Fig. 5) originate laterally at the clypeolabral connecting area. They bear small mesal extensions. A heart-shaped brush of short microtrichia (epb, Fig. 5) is present in the central epipharyngeal region. The remaining epipharyngeal surface is sculptured but lacks setae. The lateral margin between the membranous anterior epipharynx and the sclerotized labrum bears several

long setae. Disto-mesally this margin is membranous and densely covered with small setae.

3.5. Mandibles
Fig. 6

The dicondylic mandibles are strongly sclerotized and approximately one third as long as the head capsule. They are as long as broad at the base and moderately flattened. The lateral margins are rounded whereas the mesal edges are straight and interact with each other. Some setae are inserted dorso-laterally and meso-proximally. Distally the left mandible bears a larger apical and a smaller subapical tooth (I, II, Fig. 6). Both incisivi lie approximately on the same level and continuous ridges are present along their ventral margins. The anterior end of the mesal cutting edge (mr1, Fig. 6) lies above the subapical incisivus. It extends over nearly half the mandibular length and reaches a dent-like mesal protuberance (mpr, Fig. 6). From there the short second part of the cutting edge (mr2, Fig. 6) continues dorso-anteriorly. It ends at the distal edge of the oval mola (mo, Fig. 6), which is approximately twice as long as wide. The dorsal surface of the mola is characterized by cuticular spines arranged in groups. Ventrally it is confined by a strongly sclerotized ridge. A row of setae is inserted on the dorsal edge. The mandibular area above the mola shows a scale-like surface structure. Strong abrasions are visible in older specimens (Fig. 6D,E,F).

The right mandible is similar in its general configuration and shape but slightly shorter. The apical tooth is less widely separated from the subapical one. The mesal cutting edge ends in the mesal protuberance without a dorso-distal part. The mesal protuberance is not as prominent as on the left mandible.

3.6. Maxillae
Figs. 7, 8

The maxillae are about as high as broad and approximately four times as long as broad, as a whole about two thirds as long as the head capsule. The cardinal sclerite (CA, Figs. 1, 2) is sparsely covered with setae and shares the disti- (dc, Fig. 8) and the basicardo (bc, Fig. 8). In between is a prominent cardinal ridge. The long tendon of M37 arises from the basicardo. In between the disticardo and stipital sclerite (ST, Figs. 1, 2, 7) is a narrow membranous syndesis and a tiny ventral ball-and-socket-joint. The stipital ridge begins disto-mesally on the ventral surface of the stipital sclerite and continues baso-laterally. In the middle region of the sclerite it reaches its lateral edge where it is sharply bent mesad and ends ventromesally at the cardo. It subdivides the stipital sclerite in three triangular areas: the disto-lateral dististipes (ds, Fig. 8), the mesostipes (ms, Fig. 8) and the baso-lateral basistipes (bs, Fig. 8). The large palpifer (pa, Fig. 8) is separated from the stipital sclerite by a very thin membranous
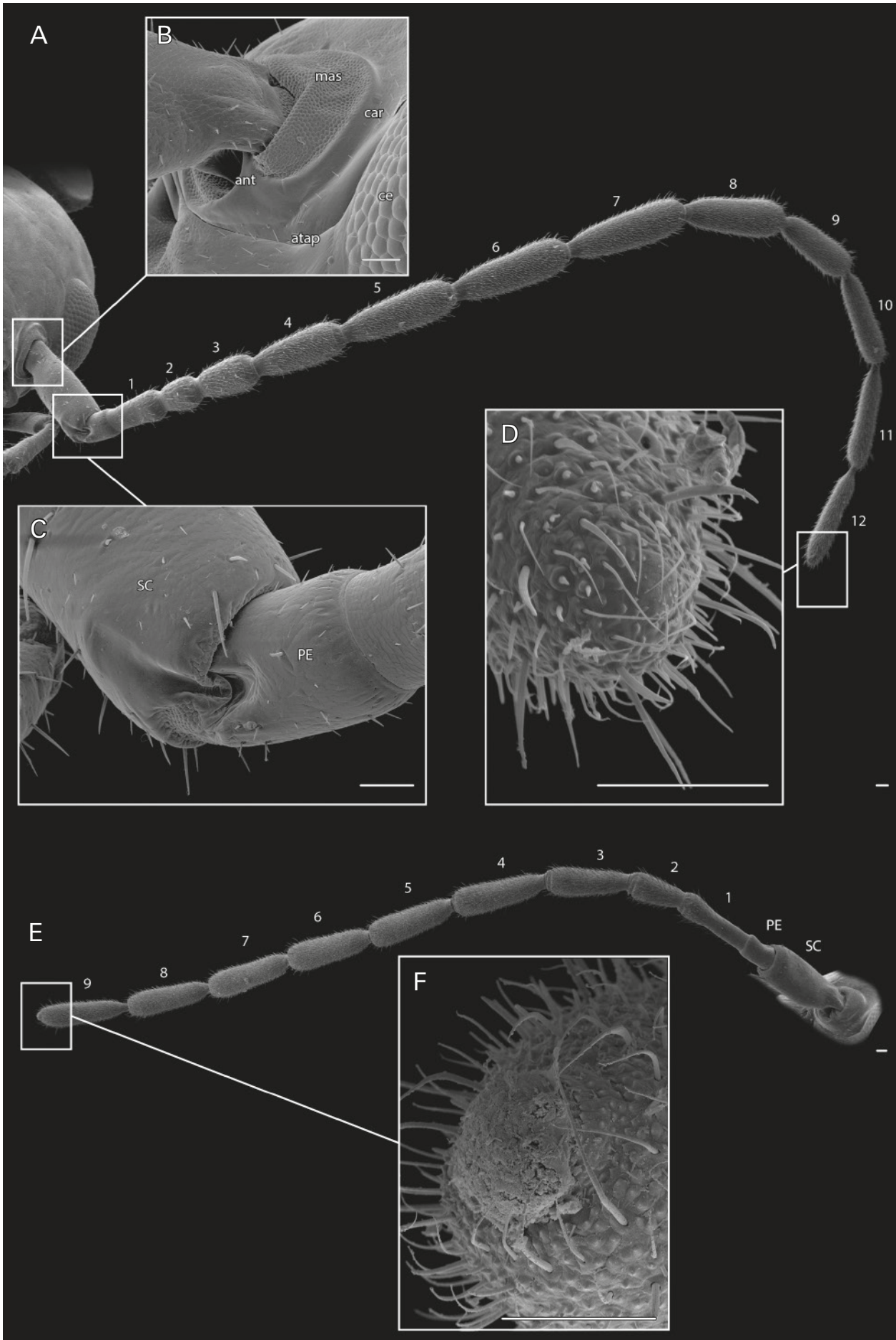
stripe and extends along its entire lateral edge. The basal palpomere articulates with its distal edge. Basally it reaches the cardo and is separated from it by a narrow membranous zone.

The maxillary palpus (mp, Figs. 1, 2) is five-segmented. The density of its setation increases distally. Palpomeres one and two are approximately as long as wide and sparsely covered with setae. Palpomeres three to five are elongated and each of them approximately four times as long as wide. The setation on the distal segment is very dense. A papilla is inserted apically (Fig. 7C).

The lacinia (la, Figs. 1, 2, 7, 8, 13) is adjacent with the disto-lateral dististipes and shows on its base near the galea a small stipital disk (sd, Figs. 8). Between lacinia and stipital ridge they are connected by a ball-and-socket-articulation. The lacinia is a sickle-shaped structure formed by a single strongly sclerotized element. Mesally it is separated from the stipital sclerite by a membranous syndesis, which allows meso-lateral movements of the lacinia. A row of long setae is present along the dorsal side of its mesal edge. In the distal quarter a second row is present on the ventral side (Fig. 7D). Apically the lacinia ends with two strongly sclerotized incisivi placed on the same level. A galeal pouch for reception of the lacinia is absent.

The galea (ga, Figs. 1, 2, 7, 8, 13) is cylindrical, approximately five times as long as wide and slightly bent mesad. It is slightly shorter than the lacinia. Its ventral side is formed by a single sclerite. It is connected with the dististipes, slightly proximad the connection with the lacinia. The mesal, distal and dorsal regions of the galea are membranous. A field of scale-like setae is present on the distal part of the membranous area (Fig. 7D).

3.7. Labium
Figs. 9, 10

The labium forms the ventral closure of the oral cavity. It is posteriorly adjacent with the gula and laterally flanked by the maxillae. It comprises the submental sclerite (SM, Figs. 1, 2, 9, 13), the mental sclerite (M, Figs. 1, 2, 9, 13), the praementum (pm, Figs. 1, 2, 9, 13) with four praemental sclerites (BPM, DPM Fig. 10), the palpiger (PG, Figs. 10, 11), the three-segmented palpus (lp, Figs. 1, 2) and the paired paraglossae (pgl, Figs. 1, 2, 9–13). The submental sclerite is a plate-like structure. It is approximately as long as wide. Distally it narrows slightly, with a concave anterior margin, which is adjacent with the mental sclerite. Posteriorly it is separated from the gula by a narrow membrane. Like the other labial parts it bears few isolated setae. The mental sclerite is much less
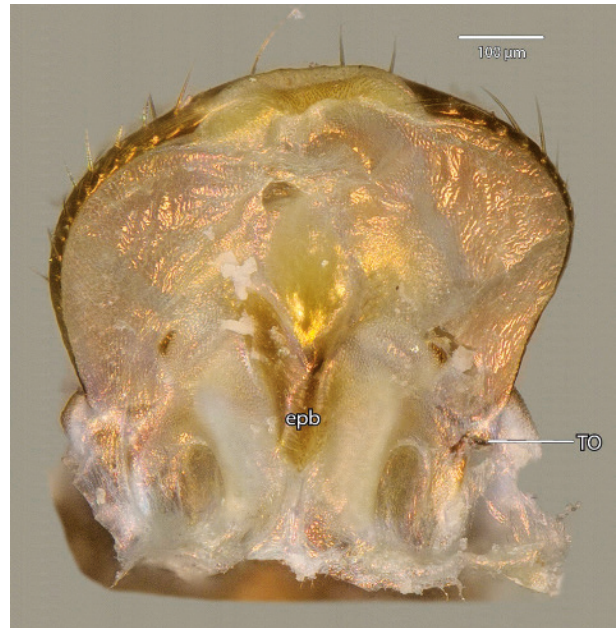

Fig. 5. *Forficula auricularia*, epipharynx, digital photography. Ventral view. — *Abbreviations*: epb – epipharingeal brush; TO – tormae.

sclerotized than the submental one. Laterally the degree of sclerotization decreases continuously. The praementum is completely divided by a deep median incision. It contains two paired sclerites basally and distally. The triangular basal sclerites (BPM, Fig. 10) are located on each side of the praemental incision. Distally, well separated from the basal sclerites by membranous areas the distal praemental sclerites (DPM, Fig. 10) are positioned. Laterally to each basal praemental sclerites, a palpiger (PG, Figs. 10, 11) is attached. It is not connected to the praemental sclerites but well separated by membranes. Distal to the palpiger, the labial palpus is attached. It is separated from the praemental sclerites and the palpiger by membranes. The palpus is three-segmented with a short and nearly squared basal palpomere (1, Figs. 9, 10). The second one is three times as long as wide (2, Figs. 9, 10). The distal palpomere is densely covered with setae and twice as long as wide (3, Figs. 9, 10). Distally it is membranous and a papilla is present on the apical region (Fig. 9B).

The paired paraglossae insert on the anterior praemental margin, connected with the distal praemental sclerites by articulatory membranes. They are sclerotized proximally, with a continuously decreasing sclerotization towards the membranous distal region. Its mesal surface bears a dense brush of setae whereas setae are sparsely distributed on the remaining parts. A distinct membra-

← **Fig. 4.** *Forficula auricularia*, left antennae, scanning electron micrographs. **A**: dorsofrontal view; **B**: joint head capsule-scapus, lateral view; **C**: joint scapus-pedicellus, dorsofrontal view; **D**: tip of last flagellomere, lateral view; **E**: left antennae of another individual with incomplete flagellomere, lateral view; **F**: tip of breaking point at ninth flagellomere, frontal view. — *Abbreviations*: ant – antennifer; atap – anterior tentorial pit; car – circumantennal ridge; ce – compound eyes; mas – membrane of the antennal socket; PE – pedicellus; SC – scapus. — Scale bar: 50 μm.
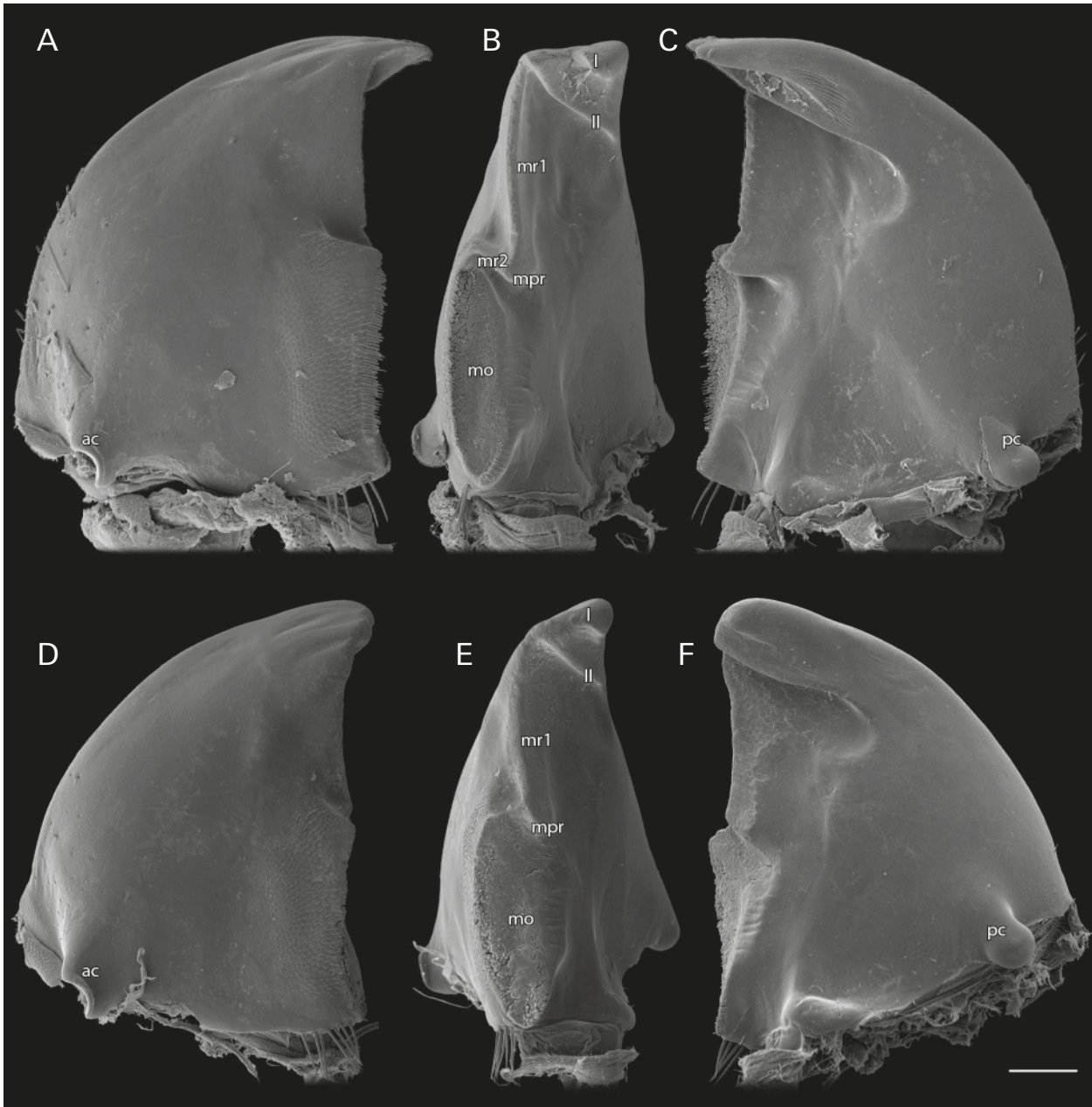
Fig. 6. *Forficula auricularia*, mandible, scanning electron micrographs. **A**: left mandible, dorsal view; **B**: left mandible, median view; **C**: left mandible, ventral view; **D**: left mandible, other individual, dorsal view; **E**: left mandible, other individual, median view; **F**: left mandible, other individual, ventral view. — ***Abbreviations***: ac – anterior condyle of the mandible; mo – mandibular mola; mpr – mesal protuberance; mr1 – mesal ridge 1; mr2 – mesal ridge 2; pc – posterior condyle of the mandible. — Scale bar: 200 μm.

nous bulge, the bumpulus (bu, Fig. 10), is present distally. Its median region is covered with spatulate setae (Fig. 9C).

3.8. Hypopharynx
Figs. 11, 12

The flexible, tongue-like hypopharynx (hyp, Figs. 11, 12) forms the posteroventral wall of the cibarium and a slope towards the anatomical mouth opening. It is located dorsally on the labium from which it is distally separated by the salivarium. The hypopharynx bears a distal lateral lobe on each side (llo, Figs. 11, 12). It is approximately as broad as the praementum and half as long as the entire labium. The dorsal surface is densely covered with microtrichia that are short and spatulate on the distal region (fch1, Figs. 11, 12) but long and hair-like closer to the anatomical mouth opening (fch2, Figs. 11, 12). Several sclerotized elements are embedded in the more or less membranous or semimembranous main body of the hypopharynx. They can be divided into anterior lingual sclerites and posterior suspensorial sclerites. The paired lateral lingual sclerites (LLS, Figs. 11, 12) in the lateral hypopharyngeal wall reach far posteriorly. They are confluent with the ventral lingual sclerites (VLS, Figs. 11,
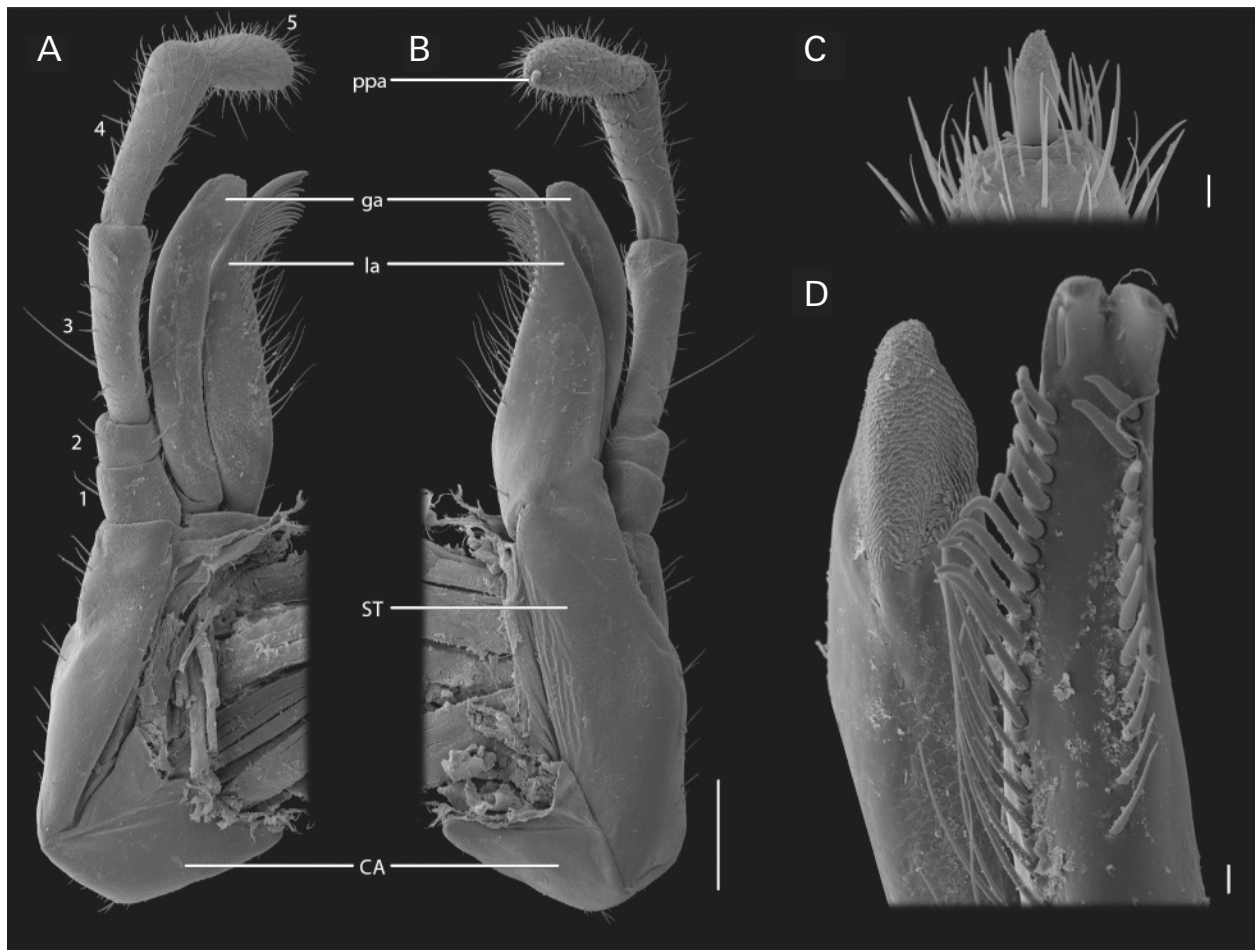
Fig. 7. *Forficula auricularia*, left maxilla, scanning electron micrographs. **A**: dorsal view; **B**: ventral view; **C**: tip of maxillary palpus, ventrolateral view; **D**: galea and lacinia, median view. — ***Abbreviations***: CA – cardinal sclerite; ga – galea; la – lacinia; ppa – palpus papillae; ST – stipital sclerite. — Scale bar: 200 μm.

12) at their terminal region, which continue disto-ventrally to form the sclerotized floor of the hypopharynx. In between them is a row of middle long setae. Dorsally, the lateral lingual sclerite is connected to the arm-like distomesal part of the suspensorium, (SMP, Figs. 11, 12) which meet the opposite distomesal part in between the two microtrichia fields fch1 and fch2. On the left side of the hypopharynx behind the arm-like distomesal part of the suspensorium is the dorsal lingual sclerite (DLS, Figs. 11, 12). Posterio-dorsally, the lateral lingual sclerite is connected to the plate-like distal part of the suspensorium (SDP, Figs. 11, 12). It is less elongated posteriorly than the lateral lingual sclerite. Postero-dorsally the oral arm (SOA, Figs. 11, 12) of the suspensorium attaches to the plate-like suspensorial part. It is a long and slender bar which continues dorsally. The anatomical mouth opening is enclosed by these oral arms. The sickle-shaped and posteriorly narrowing loral arm of the suspensorium (SLA, Figs. 11, 12) is inserted close to the connecting region of the plate-like suspensorial part and the oral arm. It continues below the membrane and forms an internal apodeme within the hypopharynx. Posteriorly it is separated from the oral arm by a very narrow membranous area, whereas both elements are confluent anteriorly. The salivarium is

a pocket below the postero-ventral part of the hypopharynx. The salivary ducts do not enter the salivarium but open on the membrane between the submentum and the maxilla. The mandibular glands release their secretions into the cibarium through an opening positioned laterally of the oral arms (omg, Fig. 11). Linguactual arms or sclerites laterad the oral arms are not present.

3.9. Pharynx
Fig. 3

The pharynx is a uniform tube and round in cross section, with a diameter of about one sixth of the width of the head capsule. Its interior surface is covered with small plicae to increase the surface. These plicae are at maximum one fourth in the length of the radius of the pharynx.

3.10. Cephalic central nervous system
Fig. 3

The main part of the moderately sized brain or supraoesophageal ganglion (sog, Fig. 3) lies between the com-

Fig. 8. *Forficula auricularia*, left maxilla, digital photography. **A**: median view; **B**: ventral view; **C**: lateral view. — ***Abbreviations***: bc – basicardo; bs – basistipes; dc – disticardo; ds – dististipes; ga – galea; la – lacinia; ms – mesostipes; pa – palpifer; sd – stipital disk; sr – stipital ridge.

pound eyes. The subdivision into proto-, deuto- and tritocerebrum is not recognizable externally but only indicated by the origin of specific nerves. The optic lobes (lopt, Fig. 3) and the antennal nerves (nant, Fig. 3) are well developed. The nervus connectivus originates anterio-mesally from the tritocerebral part of the brain and connects it with the frontal ganglion (fgl, Fig. 3) directly above the anatomical mouth. The nervus reccurens originates from the posterior end of the frontal ganglion and reaches the hypocerebral ganglion posteriorly (hyggl, Fig. 3). The nervus labralis originates from the tritocerebrum and innervates the labrum. The short circumoesophageal connectives connects the brain with the suboesophageal ganglion (soes, Fig. 3). A tritocerebral commissure is present as a separate structure below the pharynx. The suboesophageal ganglion is much more slender than the brain.

3.11. Cephalic musculature
Figs. 11, 13, 14, 15, 16

The origin, insertion and number of all cephalic muscles are shown in Table 2 and they are illustrated in figures 11 and 13 – 16.

4. Discussion

4.1. Comparison with earlier works

The present study is the first complete treatment of the external and internal cephalic morphology of *Forficula auricularia*, even though parts of the head were already
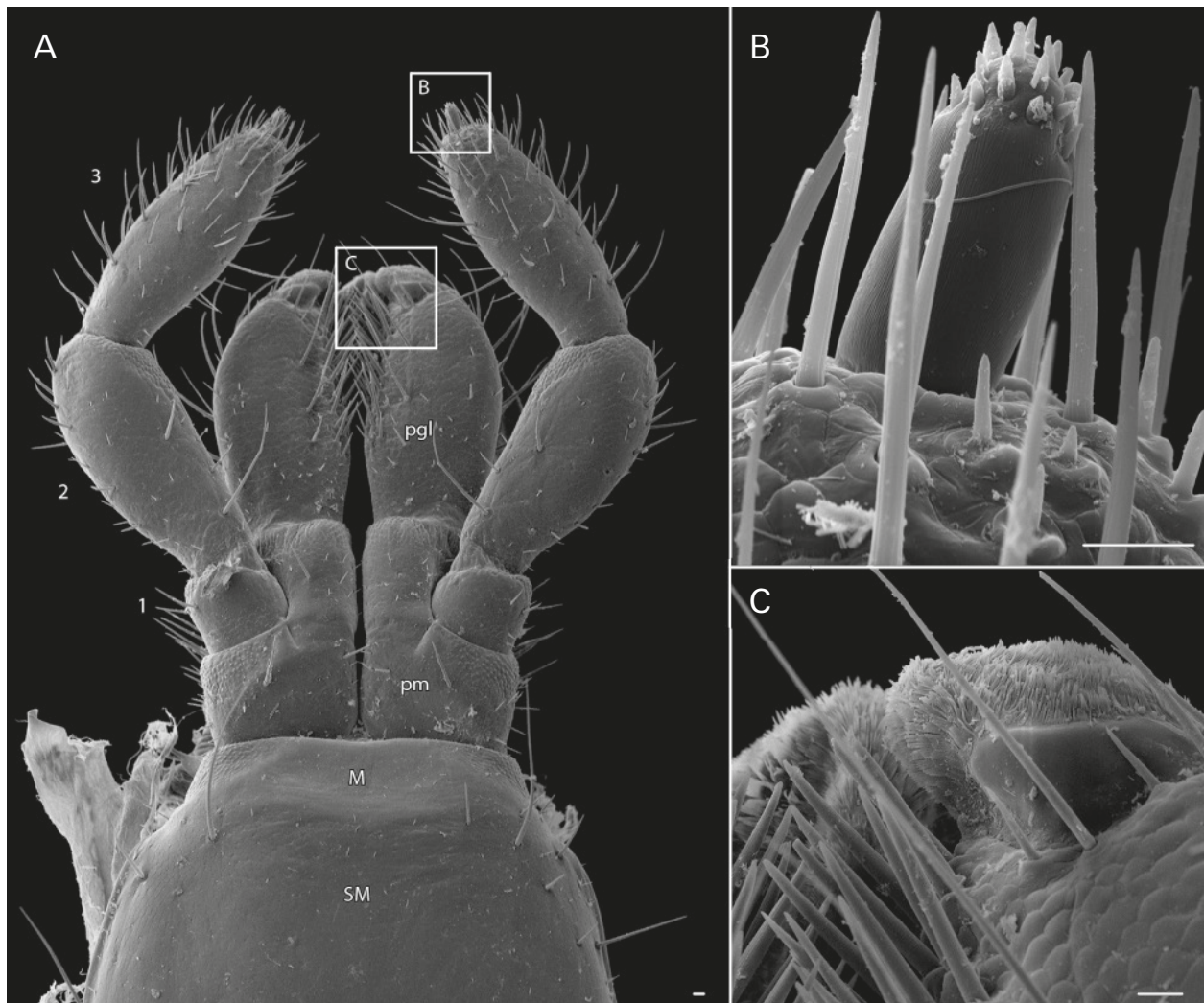
Fig. 9. *Forficula auricularia*, labium, scanning electron micrograph. **A**: ventral view; **B**: tip of labial palpus, dorsal view; **C**: tip of paraglossa, ventral view. — ***Abbreviations***: M – mental sclerite; pgl – paraglossa; PM – praemental sclerite; SM – submental sclerite. — Scale bar: 10 µm.

described in a number of previous works. The head capsule and the mouthparts were studied by WALKER (1933), STRENGER (1950), HENSON (1950), POPHAM (1959) and WALLER et al. (1996). WALKER (1931) studied the clypeus and the labrum and MOULINS (1969) the hypopharynx. PASS (1988) provided a detailed treatment of the antennal heart. The nervous system was described by KÜHNLE (1913) and the antennal sensory organs by SLIFER (1967).

Our results concerning the head capsule do largely conform with previous findings, with some noteworthy exceptions. The descriptions in previous studies were restricted to external features and did not cover the strengthening ridges associated with the coronal and frontal cleavage lines. In the following discussion, we only focus on differences that are explicitly mentioned by previous authors and not on omitted details. Differences in the terminology will not be addressed either.

POPHAM (1959) described a "temporal suture" running from the postero-dorsal edge of the compound eyes across the head capsule towards the parietal ridge (Popham´s occipital suture). This suture or ridge was not observed in the specimen studied here nor reported by any other author.

Various numbers of antennal flagellomeres are reported for *Forficula auricularia*. We observed an adult antenna with scapus, pedicellus and a flagellum with twelve flagellomeres in agreement with SLIFER (1967). SLIFER (1967) studied 188 individuals and found none with more than twelfe flagellomeres. However, 120 of them had less than twelfe, a condition due to injury or failure to develop all flagellomeres according to the author. Our study confirms this tendency to loose distal flagellomeres and illustrates a typical scar, which remains after the loss (Fig. 4). In contrast to these findings STRENGER (1950) and KLAUSNITZER & SCHIEMENZ (2010) reported different findings, the former scapus, pedicellus, and 15 uniform segments ("Auf den Scapus folgt der kleinere Pedicellus, der dann die 15 gleichförmigen Glieder der Antenne trägt") but the latter 15 segments including scapus and pedicellus. The joint between the scapus and the pedicellus (Fig. 4C) was not mentioned by any previous author.

**Table 2.** Cephalic musculature of *Forficula auricularia*.

	Origin	Insertion
M1	medially between the compound eyes on frons	medially on outer basal wall of labrum
M2	frons, mesally of the antennal base	tormae
M3	outer labral wall	epipharynx
M4	vertex near coronal ridge	dorsolateral wall of pharynx, lateral to hypocerebral ganglion
M5	posterior tentorial arms	ventrolateral wall of pharynx
M6	postclypeus, posterior to M10	dorsolateral wall of pharynx, in between anatomical mouth and frontal ganglion
M7	frons, posterior epistomal ridge	dorsolateral wall of pharynx, posterior to frontal ganglion
M8	frons, between frontal ridge and epistomal ridge	dorsolateral wall of pharynx, directly anterior to supraoesophageal ganglion
M9	on corpotentorium, dorsal and anterior tentorial arms	lateral wall of pharynx
M10	postclypeus	roof of cibarium
M11	anterior dorsal arm, corpotentorium	ventral basal margin of scape
M12	dorsal tentorial arm	dorsal basal margin of scape
M13	dorsal tentorial arm	lateral basal margin of scape
M14	between anterior and dorsal tentorial arms	mesal basal margin of scape
M15	dorsolateral wall of scape	dorsal wall of pedicel
M16	ventral wall of scape	ventral edge of pedicel
M17	frons	oral arms of the suspensorial sclerites
M18	submentum	hypopharyngeal apodeme
M19	corpotentorium	suspensorium of the hypopharynx close to oral arm
M20	distolateral wall of praementum, close to paraglossa	lateral wall of salivarium
M21	frons close to epistomal ridge	oral arms of the suspensorial sclerites
M22	basal part of praementum	lateral wall of salivarium
M23	inner edge of basicardo	laterobasal edge of praementum
M24	posterior tentorial arms	paraglossa, close to labial palp
M25	mediocentral part of submentum	mediobasal edge of praementum
M26	mesal on the basal edge of praementum	dorsobasal edge of paragloassa
M27	lateral on praementum	ventral edge of the labial palpus
M28	basal edge of praementum	lateral edge of the labial palpus
M29	dorsomedial basal edge of labial palpomere 1	dorsal basal edge of labial palpomere 2
M30	ventromedial basal edge of labial palpomere 1	ventral basal edge of labial palpomere 2
M31	lateral basal edge of labial palpomere 2	lateral basal edge of labial palpomere 3
M32	mesall basal edge of labial palpomere 2	mesal basal edge of labial palpomere 3
M33	vertex and coronal ridge	tendon that inserts at the median edge of mandible
M34	vertex and parietal ridge	tendon that inserts at the lateral edge of mandible
M35	anterior tentorial arm	ventral basal margin of mandible
M36	anterior tentorial arm	dorsal basal margin of mandible
M37	parietal ridge, vertex	basal cardinal process, basicardo
M38	posterior head capsule, vertex	basal mesal edge of lacinia, shares the tendon with M42
M39	corpotentorium	complete cardo
M40	corpotentorium	anterior on stipes, stipital ridge
M41	corpotentorium	basally on stipes, stipital ridge
M42	lateral wall of stipes	basal mesal edge of lacinia, shares the tendon with M38
M43	basal wall of stipes	basal lateral edge of galea
M44	stipital ridge	in two bundles. One basally and one distally on basal edge of maxillary palpomere 1.
M45	stipital ridge	distally at the basal edge of maxillary palpomere 1
M46	ventral basal edge of maxillary palpomere 1	ventral basal edge of maxillary palpomere 2
M47	dorsal basal edge of maxillary palpomere 1	dorsal basal edge of maxillary palpomere 2
M48	ventral basal edge of maxillary palpomere 2	ventral basal edge of maxillary palpomere 3
M49	dorsal basal edge of maxillary palpomere 2	dorsal basal edge of maxillary palpomere 3
M50	ventral basal edge of maxillary palpomere 3	ventral basal edge of maxillary palpomere 4
M51	dorsal basal edge of maxillary palpomere 3	dorsal basal edge of maxillary palpomere 4
M52	mesal basal edge of maxillary palpomere 4	dorsal basal edge of maxillary palpomere 5
M53	lateral basal edge of maxillary palpomere 4	ventral basal edge of maxillary palpomere 5
M54	oral arm of suspensorial sclerite	oral arms of suspensorial sclerites on other side
M55	ventral labral wall	ventral labral wall of other side
M56	ring muscle layer that covers the entire pharynx	
M57	longitudinal muscle layer directly above M56	
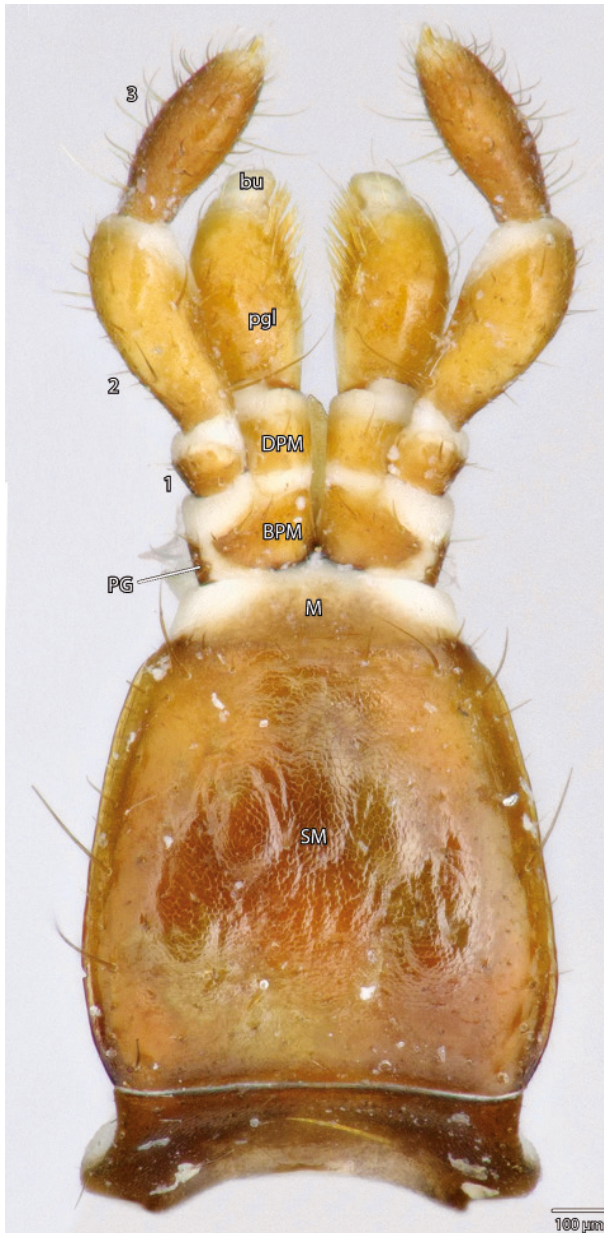
Fig. 10. *Forficula auricularia*, labium, digital photography. Ventral view. — ***Abbreviations***: bu – bumpulus; M – mental sclerite; PG – palpiger; pgl – paraglossa; BPM – basopraemental sclerite; DPM – distopraemental sclerite; SM – submental sclerite. — Scale bar: 10 µm.
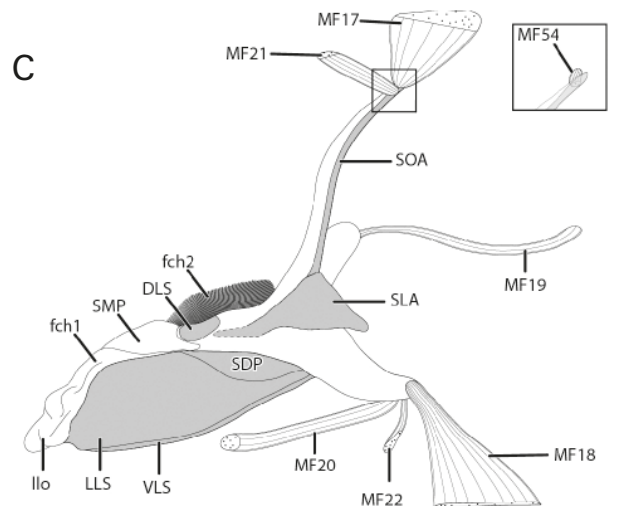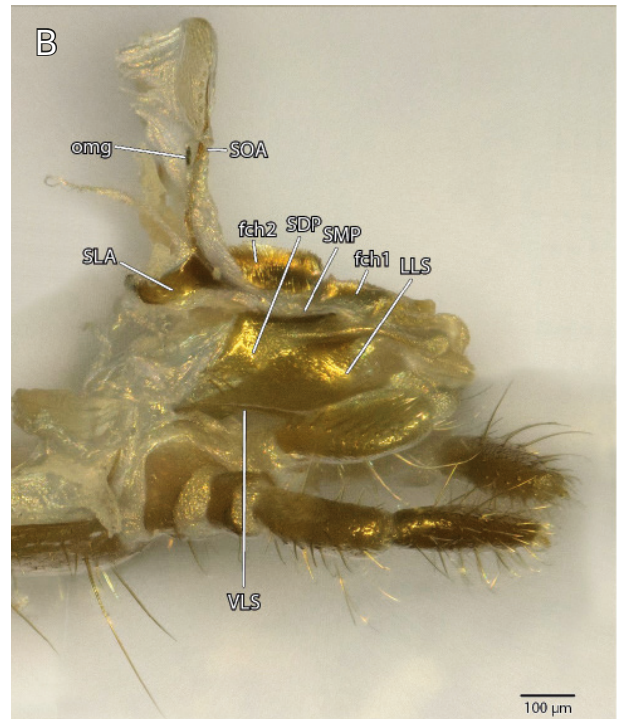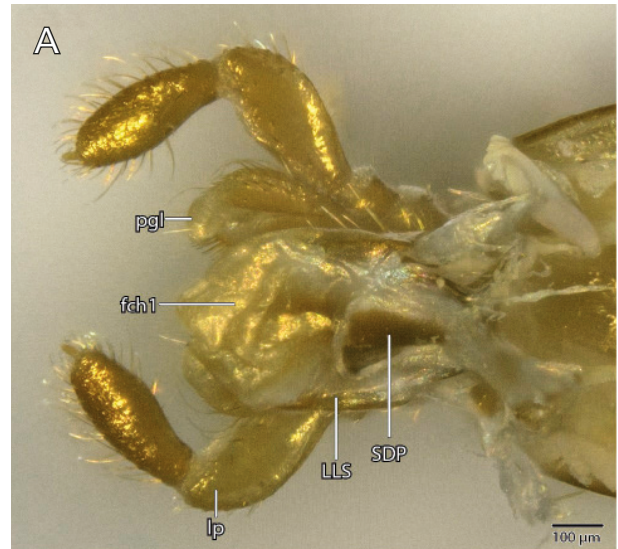
→ **Fig. 11.** *Forficula auricularia*, hypopharynx. **A**: dorsal view, digital photography; **B**: lateral view, digital photography; **C**: musculature of hypopharynx, lateral view, line drawing. — ***Abbreviations***: DLS – dorsal lingual sclerite; fch1 – sensory field with short and spatulate sensillae; fch2 – sensory field with long and hair-like sensillae; llo – lateral lobe; LLS – lateral lingual sclerite; lp – labial palpus; omg – opening of mandibular gland; PG – palpiger; pgl – paraglossa; SDP – plate like distal part (suspensorium); SLA – loral arm (suspensorium); SMP – arm-like distomesal part of the suspensorium; SOA – oral arm (suspensorium); VLS – ventral lingual sclerite.
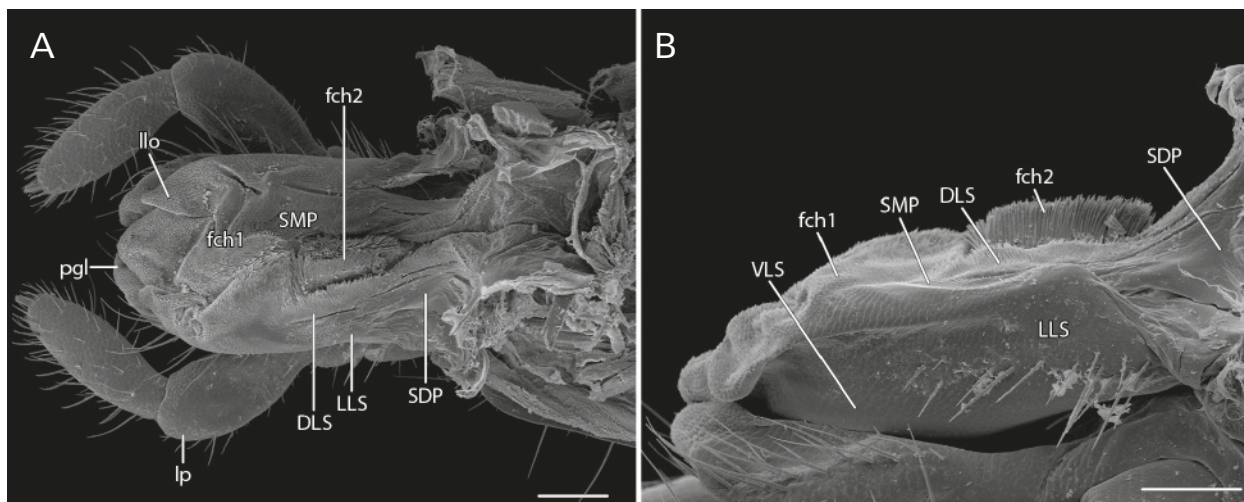
Fig. 12. *Forficula auricularia*, hypopharynx, scanning electron micrographs. **A**: dorsal view; **B**: lateral view. — ***Abbreviations***: DLS – dorsal lingual sclerite; fch1 – sensory field with short and spatulate sensillae; fch2 – sensory field with long and hair-like sensillae; llo – lateral lobe; LLS – lateral lingual sclerite; lp – labial palpus; pgl – paraglossa; SDP – plate like distal part (suspensorium); SMP – arm-like distomesal part of the suspensorium; VLS – ventral lingual sclerite. — Scale bar: 100 μm.

In her description of the mandible STRENGER (1950) mentioned a smooth mola. However, in agreement with POPHAM (1959), we observed a dorsal part of the mola composed of dense microtrichia (Fig. 6). The lacinia of *Forficula* bears two rows of setae (Fig. 7D), even though POPHAM (1959), GILES (1962) and WALLER et al. (1996) only described a single one. STRENGER (1950) mentions a three-segmented maxillary palpus, apparently an oversight as she illustrated five palpomeres.

The distal lobe of the labium was discussed controversially. STRENGER (1952) considered it as the glossae whereas HAAS (2005) referred to it as a product of fusion of glossae and paraglossae. However, the presence of M. tentorioparaglossalis and M. praementoparaglossalis clearly indicates that the paraglossae are still present. Additionally, there is a trend in polyneopteran insects to reduce the size of the glossae. We therefore follow POPHAM (1959), GILES (1962), MATSUDA (1965) and others by assuming that the glossae were reduced.

POPHAM (1959) illustrated three pairs of hypopharyngeal sclerites and the position and arrangement differs from our observation. His basal sclerite might be our loral arm of the hypopharyngeal suspensorium, his median sclerite the plate-like part of the suspensorium, and his distal sclerite our lateral lingual sclerite. However, as POPHAM (1959) did not provide a lateral view, a reliable homologation is not possible. The description of the sclerites in MOULIN (1969) is similar to our description, except the location of the loral arm of the suspensorium (SLA, Figs. 11, 12, 19). He described the location of this sclerite (sc, MOULIN 1969) on the surface of the hypopharynx but we observe that the anterior part goes under the membrane inside the hypopharynx. The salivary and mandibular gland open together on the dorso-mesal surface of the hypopharynx according to POPHAM (1959). This is in contrast to the detailed observations of MOULIN (1969) and KÜHNLE (1915), who described an opening of

the salivary ducts in the membrane between the submentum and the maxilla, and an opening of the mandibular gland laterally of the oral arms of the hypopharynx. This also confirms our observation.

The muscles of *Forficula* were described by STRENGER (1950), POPHAM (1959) and WIPFLER (2012) (Table 3). STRENGER (1950) studied those of the mouthparts and antennae, and POPHAM (1959) the musculature of the feeding apparatus. WIPFLER (2012) listed all muscles in a table but did not provide origin or insertion or any other detail. The two antennal muscles described by STRENGER (1950) cannot be clearly homologized with the four described here. Additionally, she did not mention M. tentoriostipitalis posterior and M. anularis stomodaei. In POPHAM's (1959) study M. tentoriomandibularis lateralis inferior, M. stipitolacinialis, M. tentorioparaglossalis, M. praementopalpalis internus and M. praementopalpalis externus are not mentioned. Additionally, both authors did not cover M. labralis transversalis, M. tentoriomandibularis medialis inferior, M. tentoriobuccalis, M. tentoriopharyngealis, M. postoccipitopharyngealis and the musculature of the palpi. The presence of M. hypopharyngeosalivaris (0hy12) and M. tentoriofrontalis anterior (0te2) listed in WIPFLER (2012) could not be confirmed.

From a morphological point of view *Forficula* is the best-studied earwig. However, the current study clearly shows that several previous works contradict each other and a detailed documentation of the cephalic morphology was lacking so far. Another major shortcoming of previous studies is the lack of a detailed documentation of the structural features. As erroneous or incomplete data can strongly affect phylogenetic evaluations, a detailed re-evaluation with modern techniques including a careful character documentation appeared justified to us. Interestingly a similar situation was found in the well-known cosmopolitan cockroach *Periplaneta americana*
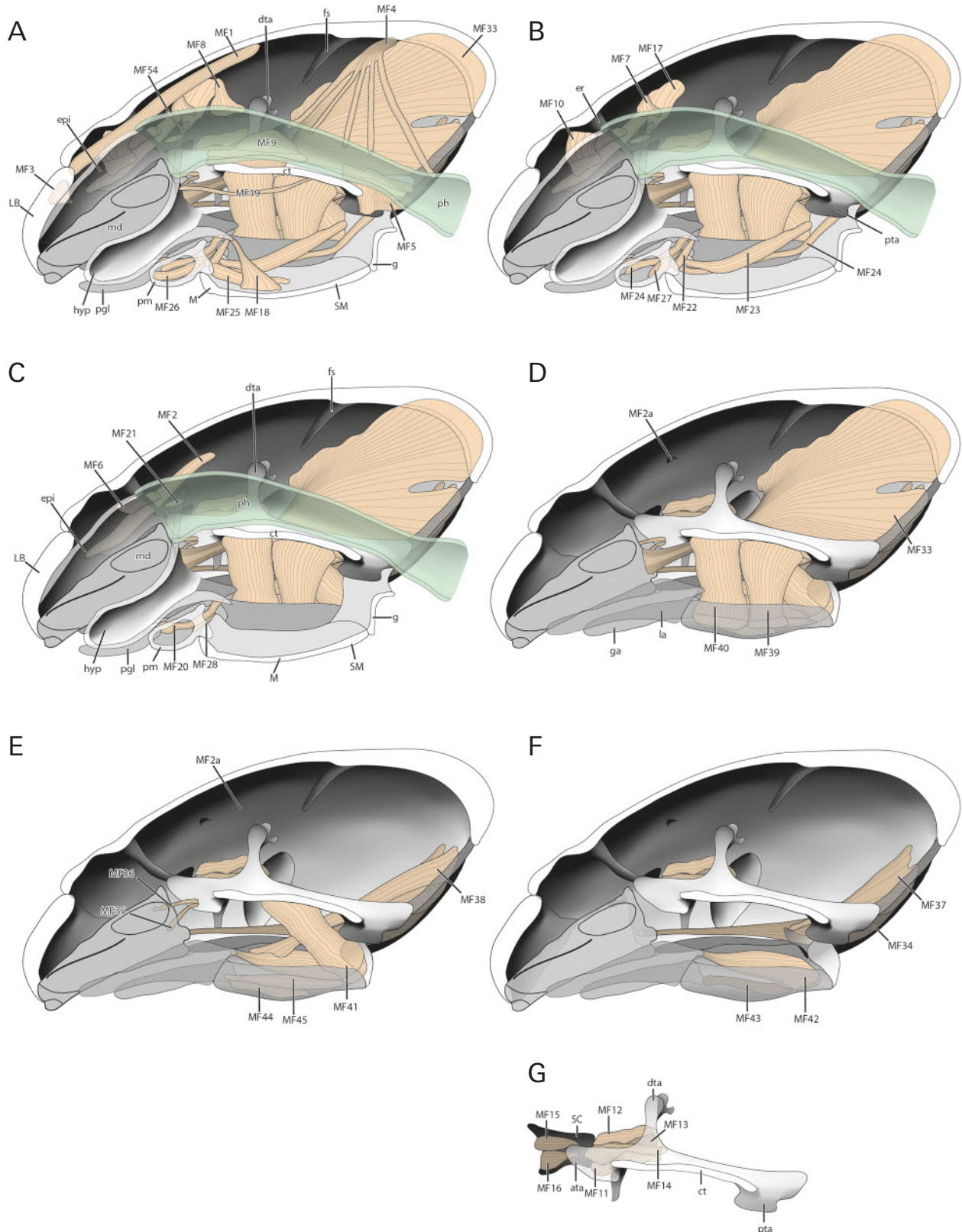
Fig. 13. *Forficula auricularia*, cephalic musculature and endoskeleton, mediosagital view, line drawings. **A**: with all layers of musculature; **B**: without muscles m1, m3, m4, m5, m9, m8, m18, m19, m25, m26, m54; **C**: without labium, digestive system, epipharynx, hypopharynx, m7, m10, m17, m22, m23, m24, m27; **D**: without muscles m2, m6, m20, m21, m28; **E**: without muscles m33, m39, m40; **F**: without muscles m35, m36, m38, m41, m44, m45; **G**: antennal muscles and tentorium without head capsule and maxillae. — ***Abbreviations***: ata – anterior tentorial arm; ct – corpotentorium; dta –: dorsal tentorial arm; epi –: epipharynx; er –: epistomal ridge; fs – frontal cleavage line; g – gula; ga – galea; hyp – hypopharynx; la – lacinia; LB – labral sclerite; M – mental sclerite; m02a – original of m02; md – mandible; pgl – paraglossa; ph – pharynx; PM – praemental sclerite; pta – posterior tentorial arm; SC – scapus; SM – submental sclerite.

(WIPFLER et al. 2016), where a reassessment of the head morphology also yielded important new information.

4.2. Evolutionary implications

The monophyly of Dermaptera is strongly supported by unsegmented and curved cerci in the adults, a highly specialized wing folding mechanism, and strongly shortened tegmina, and also in different molecular analyses (COLGAN et al. 2003; JARVIS et al. 2005; KOCAREK et al. 2013; NAEGLE et al. 2016). It is also widely accepted that Dermaptera belongs to the polyneopteran or lower neopteran insects, a phylogenetically problematic group with uncertain monophyly (see BEUTEL et al. 2014a for a review). However, the exact position within this lineage is completely unclear and almost all other groups of Polyneoptera have been proposed as potential sistertaxon (Table 1).

The head morphology of earwigs is characterized by various plesiomorphies such as the presence of biting mouthparts with dicondylic mandibles, five-segmented maxillary palpi and three-segmented labial palpi or a nearly complete set of cephalic muscles (WIPFLER et al. 2011). Additionally the dermapteran head also exhibits a surprisingly large number of apomorphic characters (summarized in Fig. 17). They include the presence of a distal, membranous lobe on the paraglossa that we termed bumpulus (YUASA 1920; GILES 1962), large distal palpilla on the terminal maxillary and labial palpomeres (GILES 1962; POPHAM 1985), a stipital ridge separating the basi-, medio- and dististipes (KADAM 1961; GILES et al. 1962), the clear division of the praementum into a basal and a distal sclerite (GILES 1962), the lack of ocelli that are present in extinct species until the early Cretaceous (NEL et al. 2012), the origin of M. tentoriohypopharyngealis (0hy4) on the submentum (KADAM 1961; GILES 1962) and the reduction of the glossae. Additionally all studied dermapterans have coronal and frontal cleavage lines which are internally forming strong strengthening ridges (GILES 1962). A similar condition is known from some dipteran larvae (e.g. WIPFLER et al. 2012b) but not from any other polyneopteran insects (e.g. YUASA 1920; WIPFLER 2012). Another interesting and strongly discussed structure of the dermapteran head are the lateral lobes on the distal hypopharynx (llo, Figs. 11, 12). Their homology with the superlinguae of apterygote insects and ephemeropteran larvae was hypothesized (e.g. POPHAM 1959; GILES 1962). However, MOULINS (1969) refuted this interpretation, pointing out the apical position in Dermaptera, in contrast to the dorso-proximal position of the lobes in apterygotes and Ephemeroptera. Moreover the superlinguae are innervated by a branch of the mandibular nerve or a separate nerve from the suboesophageal ganglion connected to the mandibular nerve. In contrast to this, the apical lobes of *Forficula* are innervated by the hypopharyngeal and maxillary nerves. This suggests that the lobes that are found in all studied dermapterans (GILES 1962) are a neoformation and thus another potential ordinal autapomorphy.

A character with unclear phylogenetic polarization is the prognathous head position found in all dermapterans (GILES 1962). This condition also occurs in several other polyneopteran lineages such as Plecoptera (HOKE 1924), Grylloblattodea (WIPFLER et al. 2011), Phasmatodea (BRADLER 2009; FRIEDEMANN et al. 2012), Isoptera (VISHNOI 1956) and Embioptera (RÄHLE 1970). It is ambiguous whether prognathism was ancestral in Polyneoptera, if this lineage is monophyletic (see BEUTEL et al. 2014a for a review). What is evident is that within Polyneoptera more than one change of the orientation of the head position must have occurred since prognathous termites evolved from orthognathous roaches (e.g. DJERNÆS et al. 2015). In any case the orientation of the head position remains ambivalent with respect to the monophyly of Dermaptera or its placement within Polyneoptera. The change of the mouthpart orientation might be the cause for several other structural modifications of the head capsule such as the presence of a gula, a ventral closure of the head. It occurs in many prognathous insects such as certain Phasmatodea (BRADLER 2009), Embioptera (RÄHLE 1970) or also Coleoptera. Besides this, prognathism might be correlated with an elongated corpotentorium (Grylloblattodea: WALKER 1931; WIPFLER et al. 2011; Plecoptera: HOKE 1924) and large and externally visible dorsal tentorial pits associated with dorsal tentorial arms broadly fused with the head capsule. The latter are found in all studied dermapterans (GILES 1962) but also in Plecoptera (HOKE 1924) and Phasmatodea (GILES 1962; FRIEDEMANN et al. 2012). Even though TILGNER et al. (1999) did not describe them for the basal phasmatodean *Timema* they are also present in this genus (pers. obs.) and therefore very likely part of the phasmatodean ground pattern. In Grylloblattodea, the dorsal arms are also broadly fused to the head capsule but an externally visible pit is absent (WALKER 1931; WIPFLER et al. 2011). In Embioptera the arms are also massive and broad, but connected to the head capsule via tonofibers (RÄHLE 1970). In orthognathous polyneopteran insects such as the roach *Periplaneta* (WIPFLER et al. 2016) the dorsal arms are usually much more fragile and do not reach the head capsule.

Forficula shows several clearly derived characters for which we currently cannot specify whether they are apomorphic for Dermaptera or only a subgroup. To this category belongs the distinct scapo-pedicellar joint that is also present in *Labidura riparia* (KADAM 1961) but not reported for any other earwig so far. Although

---

→ **Fig. 14.** *Forficula auricularia*, cephalic musculature and endoskeleton, 3d-reconstruction. **A**: antennal musculature, left side dorsal view, right side ventral view; **B**: mandibular musculature, left side dorsal view, right side ventral view; **C**: maxillary extrinsic musculature, lateral view; **D**: maxillary extrinsic musculature, mediosagittal view; **E**: maxillary intrinsic musculature, dorsal view; **F**: maxillary intrinsic musculature, ventral view. — ***Abbreviations***: ct – corpotentorium; md – mandible. — Different scales.
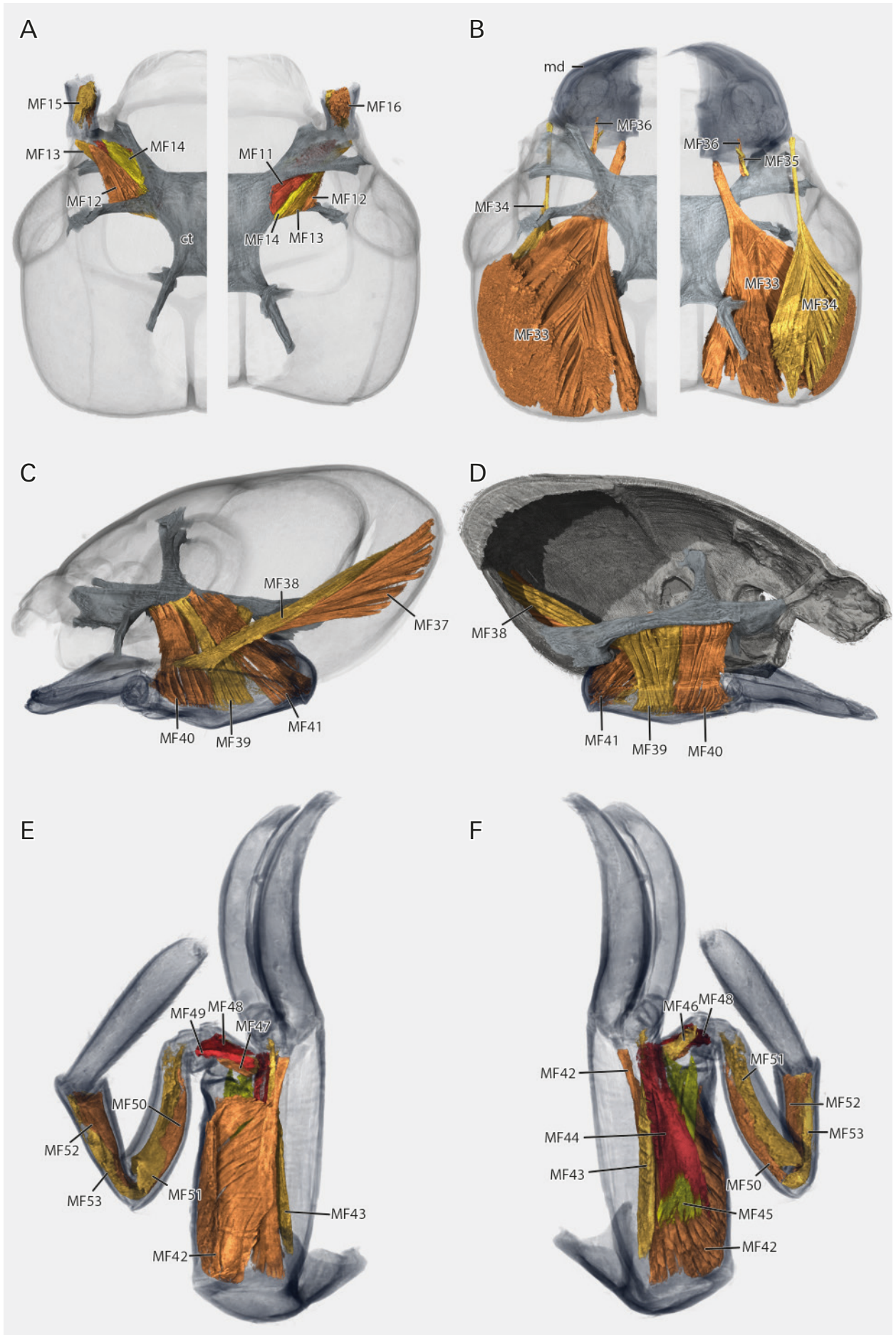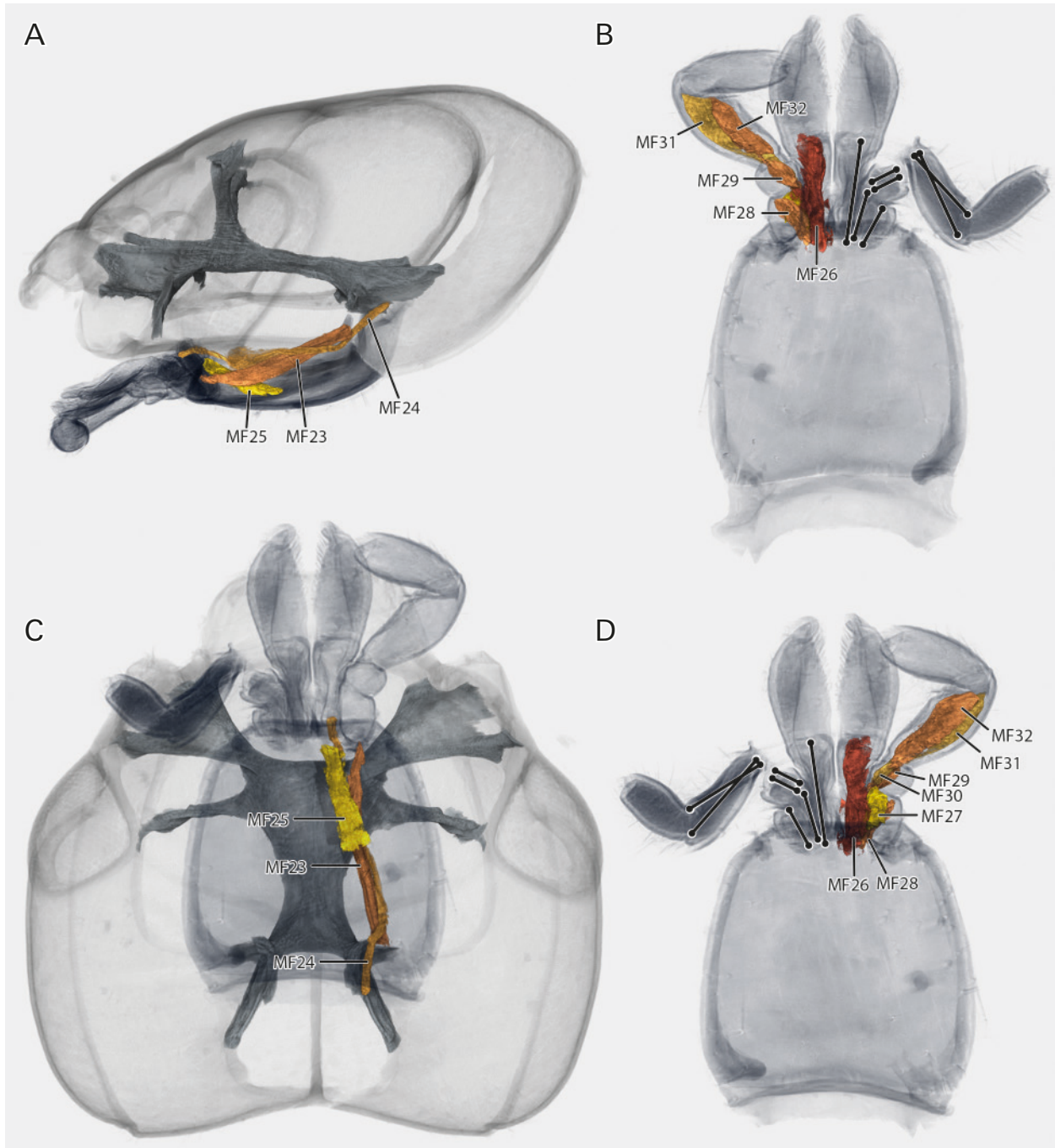
Fig. 15. *Forficula auricularia*, cephalic musculature and endoskeleton, 3d-reconstruction. **A**: selected labial muscles, lateral view; **B**: selected labial muscles, dorsal view; **C**: selected labial muscles, ventral view; **D**: selected labial muscles, ventral view. — Different scales.

articulations between the two basal antennomeres also occur in other lower neopteran groups such as Mantophasmatodea (DRILLING & KLASS 2010) and Orthoptera (GEWECKE 1972), they differ from the condition in Dermaptera, where they are large ball-and-socket joints and well visible in lateral view. Similar cases with unknown conditions in most dermapterans are the highly specialized antennal ampulla, which differs from all other polyneopteran insects by being compressed (PASS 1988; PASS et al. 2006; WIPFLER & PASS 2014), and the mandibular mola where the dorsal part is formed of coalescent spines in *Forficula*. Another feature only reported

for *Forficula* is the opening of the salivary duct in the membrane between the submentum and the maxilla. According to KADAM (1961) the salivary duct of *Labidura riparia* opens into the salivarium, as it is the case in all other studied polyneopterans, and almost generally in insects. For a reliable phylogenetic interpretation of these features, more information for other dermpaterans is required, especially for the presumably basal branches Diplatyidae, Pygidicranidae and Karschiellidae.

A long list of derived characters and potential ordinal autapomorphies stands in contrast to very few potential cephalic synapomorphies with other polyneopteran
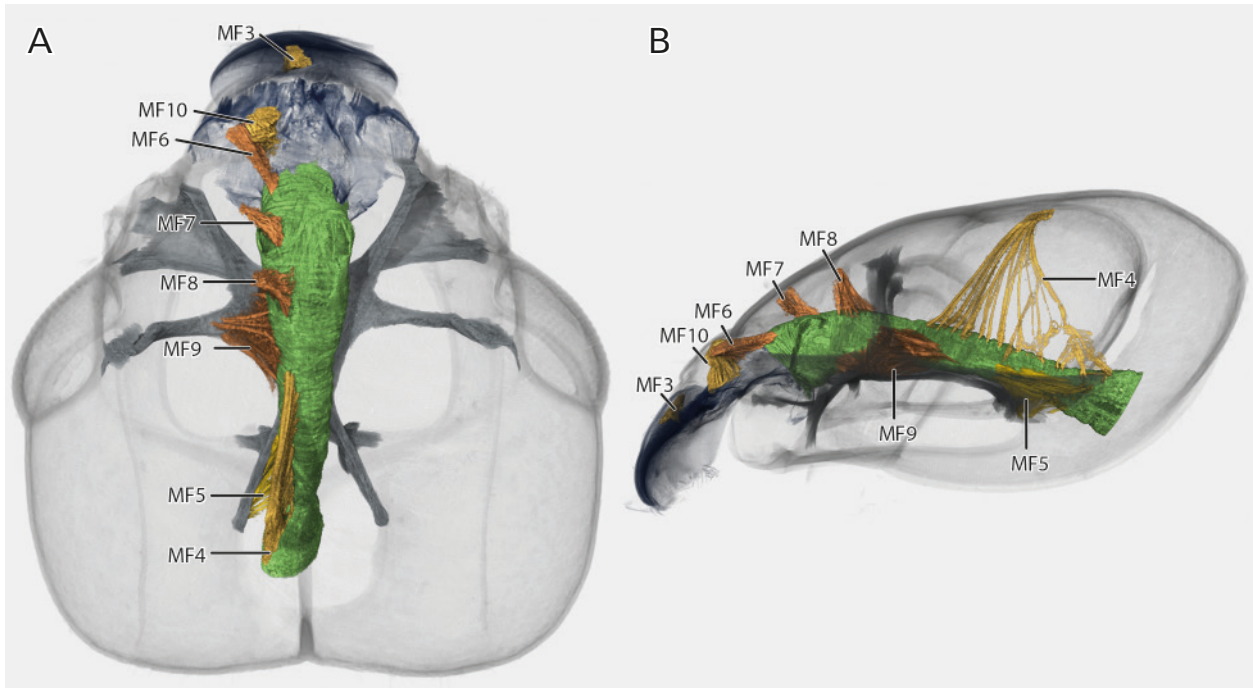
Fig. 16. *Forficula auricularia*, musculature for ingestion, 3d-reconstruction. **A**: dorsal view; **B**: lateral view. — Different scales.

Potential apomorphies for Dermaptera:
1. prognathous head position
2. presence of a gula[1]
3. strongly developed dorsal tentorial attachments areas[1]
4. corpotentorium elongated[1]
5. coronal and frontal sulci with corresponding strong internal strengthening ridges
6. lack of ocelli[2]
7. division of the prementum into a basal and a distal sclerite
8. reduction of the glossae
9. presence of a bumpulus
10. presence of large distal palpilla on the terminal maxillary and labial palpomeres
11. stipital ridge divided stipes into three subparts
12. lateral lobes on the distal hypopharynx[3]
13. origin of M. tentoriohypopharyngealis (0hy4) on the submentum

Characters with unclear distribution:
14. dorsal part of the mandibular mola is formed of coalescent cuticular spines[4]
15. antennal ampulla that are compressed[5]
16. prominent ball-and-socket joint between scapus and pedicellus[6]
17. opening of the salivary duct in the membrane between the submentum and the maxilla[7]

Potential synapomorphies with Plecoptera and/or Zoraptera:
18. absence of the linguactual tendons and the associated muscle M. hypopharyngomandibularis

[1] might be correlated with prognathism
[2] present in fossil dermapterans (NEL et al. 2012)
[3] it was discussed whether these lobes might be homologues with the superlinguae of apterygote insects and Ephemeroptera (POPHAM 1959; GILES 1962; MOULINS 1969)
[4] not described for any other dermapteran than *Forficula auricularia*
[5] present in *Forficula auricularia*, *Labidura riparia* and *Chelidurella acanthopygia* (PASS 1988) but not studied in any other earwig.
[6] only reported for *Forficula auricularia* and *Labidura riparia* (KADAM 1961)
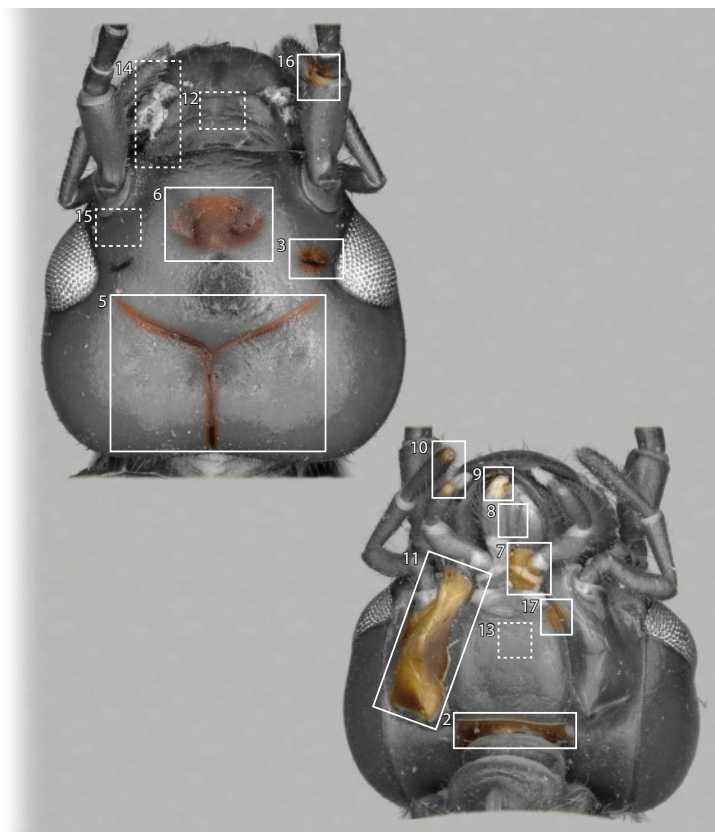
Fig. 17. Summary of the evolutionary conclusions derived from the head morphology. Illustrations provide the position of the characters (indicated by their number). Solid boxes are external characters while dotted ones imply internal ones. Additional information for each character is found in the text.

lineages (Fig. 17). A character shared with Plecoptera (CHISHOLM 1962; MOULINS 1968; BLANKE et al. 2012) and/or Zoraptera (BEUTEL & WEIDE 2005; MATSUMURA et al. 2015) is the lack of the linguactual tendons and the associated muscle M. hypopharyngomandibularis. Both groups have been considered as potential sistergroups

Table 3. Proposed homology of the musculature present in dermapterans including the general terminologies of WIPFLER et al. (2011) and v. KELÉR (1963) and the works of DORSEY (1943), STRENGER (1950), POPHAM (1959), KADAM (1961), WIPFLER (2012) and the present study. + : muscle present; – : muscle absent; / : not described in the study; ? : unclear homology.

WIPFLER et al. (2011)	WIPFLER et al. (2011)	v. KELÉR (1963)	*F. auricularia* (present study)	*F. auricularia* (STRENGER 1950)	*F. auricularia* (POPHAM 1959)	*F. auricularia* (WIPFLER 2012)	*Anisolabis maritima* (DORSEY 1943)	*Labidura riparia* (KADAM 1961)
M. tentorioscapalis anterior	0an1	1	MF11	4?	—	+	/	dp.a
M. tentorioscapalis posterior	0an2	2	MF12	5?	—	+	/	lvs
M. tentorioscapalis lateralis	0an3	3	MF13	—	—	+	/	—
M. tentorioscapalis medialis	0an4	4	MF14	—	—	+	/	—
M. scapopedicellaris lateralis	0an6	5	MF15	—	—	+	/	lv.fl
M. scapopedicellaris medialis	0an7	6	MF16	—	—	+	/	dp.f1
M. frontolabralis	0lb1	8	MF1	1	LEM	+	4	d.lr
M. frontoepipharyngalis	0lb2	9	MF2	2	LDM	+	3	v.lr
M. labralis transversalis	0lb4	—	MF55	—	—	+	?	—
M. labroepipharyngealis	0lb5	7	MF3	—	LCM	+	1	com.lr
M. craniomandibularis internus	0md1	11	MF33	MA+MB	ADM	+	/	add.md
M. craniomandibularis externus	0md3	12	MF34	25	ADM	+	—	abd.md
M. tentoriomandibularis lateralis inferior	0md6	14	MF35	26	—	+	/	—
M. tentoriomandibularis medialis inferior	0md8	14?	MF36	—	—	+	/	—
M. craniocardinalis	0mx1	15+16	MF37	6	PPM	+	/	fl.car
M. craniolacinialis	0mx2	19	MF38	9	CLF	+	/	—
M. tentoriocardinalis	0mx3	17	MF39	7	SA	+	/	add.car
M. tentoriostipitalis anterior	0mx4	18	MF40	8	SA	+	/	add.st
M. tentoriostipitalis posterior	0mx5	18	MF41	—	SA	+	/	—
M. stipitolacinialis	0mx6	20	MF42	10	—	+	/	fl.lc
M. stipitogalealis	0mx7	21	MF43	11	GF	+	/	fl.ga
M. stipitopalpalis medialis	0mx8+9	—	MF44	12	MPE	+	/	lv.plp
M. stipitopalpalis internus	0mx10	23	MF45	13	MDP	+	/	dp.plp
M. palpopalpalis maxillae primus	0mx12 / 0mx12	24 / 24	MF46 / MF47	/	—	+	/	fl2
M. palpopalpalis maxillae secundus	0mx13 / 0mx13	25 / 25	MF48 / MF49	/	—	+	/	fl3
M. palpopalpalis maxillae tertius	0mx14 / 0mx14	26 / 26	MF50 / MF51	/	—	+	/	fl4
M. palpopalpalis maxillae quartus	0mx15 / 0mx15	27 / 27	MF52 / MF53	/	—	+	/	fl5
M. tentoriopraementalis	0la5	29	MF23	15	LPA	+	21	add.pm
M. tentorioparaglossalis	0la6	30	MF24	14	—	+	20	l.re.pm
M. submentopraementalis	0la8	28	MF25	16	HDM	+	22	m.re.pm
M. praementoparaglossalis	0la11	31	MF26	20	PEM+PDM	+	29	fl.li
M. praementopalpalis internus	0la13	33	MF27	18	—	+	—	dp.plp
M. praementopalpalis externus	0la14	34	MF28	17	—	+	24	lv.plp
M. palpopalpalis labii primus	0la16 / 0la16	35 / 35	MF29 / MF30	/	—	+	?	fl2
M. palpopalpalis labii secundus	0la17 / 0la17	36 / 36	MF31 / MF32	/	—	+	?	fl.t.plp
M. frontooralis	0hy1	41	MF17	/	—	+	10	s.dl.ph?
M. tentoriooralis	0hy2	47	MF21	/	—	+	?	—
M. craniohypopharyngealis	0hy3	42	MF18	/	—	+	19	pr.hyph
M. tentoriosuspensorialis	0hy5	48?	MF19	/	—	+	—	—
M. praementosalivaris anterior	0hy7	38	MF20	/	—	+	17	v.dl.slv
M. praementosalivaris posterior	0hy8	39	MF22	/	—	+	18	—
M. oralis transversalis	0hy9	67	MF54	/	—	+	12+13?	—
M. hypopharyngosalivaris	0hy12	37	—	/	—	+	16	d.dl.slv
M. clypeopalatalis	0ci1	43	MF10	/	CDM	+	5–7	dl.cb
M. clypeobuccalis	0bu1	44	MF6	/	AOD	+	—	—
M. clypeobuccalis anterior	0bu2	45	MF7	/	MOD1	+	9	dl.b
M. clypeobuccalis posterior	0bu3	46	MF8	/	MOD2	+	11	—

Table 3 continued.

M. tentoriobuccalis	0bu4-6	49–50	MF9	/	—	+	30	—
M. verticopharyngealis	0ph1	51	MF4	/	POD	+	—	d.dl.ph
M. tentoriopharyngealis	0ph2+0ph3?	52	MF5	/	—	+	—	v.dl.ph
M. annularis stomodaei	0st1	68	MF56	/	—	+	12+13	—
M. longitudinalis stomodaei	0st2	69	MF57	/	—	+	—	—

of Dermaptera (see above). Another shared feature of Plecoptera + Dermaptera is the presence of four extrinsic antennal muscles (BLANKE et al. 2012). However, this is likely a plesiomorphic condition which is also found in the apterygote Zygentoma and Archaeognatha (BLANKE et al. 2012, 2014), and also in the holometabolous Hymenoptera (BEUTEL & VILHELMSEN 2007). In the remaining polyneopterans either M. tentorioscapalis lateralis (Embioptera, Zoraptera, Phasmatodea) or M. tentorioscapalis medialis (Dictyoptera, Grylloblattodea, Mantophasmatodea) are reduced, without a clear phylogenetic pattern. A character with unclear phylogenetic implications is the median praemental cleft. It also occurs in Grylloblattodea (WALKER 1931; WIPFLER et al. 2011), Mantophasmatodea (BAUM et al. 2007), Dictyoptera (WIPFLER et al. 2012a; WIPFLER et al. 2016), some Orthoptera (YUASA 1920) and Zorapera (BEUTEL & WEIDE 2005; MATSUMURA et al. 2015) but is unknown outside of Polyneoptera. However, its length varies strongly among these groups. In all studied Dermaptera it reaches the base of the praementum (KADAM 1961; GILES 1962), whereas it is restricted to the distal third in Grylloblattodea (WALKER 1931; WIPFLER et al. 2011) and the distal two thirds in *Periplaneta* (WIPFLER et al. 2016). For a detailed evaluation of this character and its variable length a much broader survey would be necessary.

Our study reveals an impressive number of dermapteran apomorphies, clearly outnumbering derived features occurring in other polyneopteran orders (Fig. 17). The present contribution clarifies important issues of the dermapteran head morphology. However, it also underlines the severe lack of information. The detailed study of more taxa, especially the presumably basal lineages Diplatyidae, Pygidicranidae or Karschiellidae, is essential for reconstructing phylogenetic patterns and the evolution of head structures in Dermaptera.

5. Acknowledgements

6. References

ANTONELLI M., CONTI G., MORO M.L., ESQUINAS A., GONZALEZ-DIAZ G., CONFALONIERI M., PELAIA P., PRINCIPI T., GREGORETTI C., BELTRAME F., PENNISI M.A., ARCANGELI A., PROIETTI R., PASSARIELLO M., MEDURI G.U. 2001. Predictors of failure of noninvasive positive pressure ventilation in patients with acute hypoxemic respiratory failure: a multi-center study. – Intensive Care Medicine **27**: 1718–1728.

BAUM E., DRESSLER C., BEUTEL R.G. 2007. Head structures of *Karoophasma* sp. (Hexapoda, Mantophasmatodea) with phylogenetic implications. – Journal of Zoological Systematics and Evolutionary Research **45**: 104–119.

BAYER R. 1968. Untersuchungen am Kreislaufsystem der Wanderheuschrecke (*Locusta migratoria migratorioides* R. et F., Orthopteroidea) mit besonderer Berücksichtigung des Blutdruckes. – Zeitschrift für Vergleichende Physiologie **58**: 76–135.

BEIER M. 1959. Ohrwürmer und Tarsenspinner (Dermaptera-Embioptera). – Ziemsen, Wittenberg.

BERENBAUM M. 2007. Lend me your earwigs. – American Entomologist **53**: 196.

BEUTEL R.G., FRIEDRICH F., GE S.Q., YANG X.K. 2014b. Insect Morphology and Phylogeny. – De Gruyter, Berlin. 516 pp.

BEUTEL R.G., GORB S.N. 2006. A revised interpretation of the evolution of attachment structures in Hexapoda with special emphasis on Mantophasmatodea. – Arthropod Systematics & Phylogeny **61**: 3–35.

BEUTEL R.G., VILHELMSEN L. 2007. Head anatomy of Xyelidae (Hexapoda: Hymenoptera) and phylogenetic implications. – Organisms, Diversity, Evolution **7**: 207–230.

BEUTEL R.G., WEIDE D. 2005. Cephalic anatomy of *Zorotypus hubbardi* (Hexapoda: Zoraptera): new evidence for a relationship with Acercaria. – Zoomorphology **124**: 121–136.

BEUTEL R.G., WIPFLER B., GOTTARDO M., DALLAI R. 2014a. Polyneoptera or "Lower Neoptera" – new light on old and difficult phylogenetic problems. – Atti Accademia Nazionale Italiana di Entomologia **61**: 133–142.

BEUTEL R.G., ZIMMERMANN D., KRAUSS M., RANDOLF S., WIPFLER B. 2010. Head morphology of *Osmylus fulvicephalus* (Osmylidae, Neuroptera) and its phylogenetic implications. – Organisms, Diversity, Evolution **10**: 311–329.

BLACKITH R.E., BLACKITH R.M. 1967. The anatomy and physiology of the morabine grasshoppers III. Muscles, nerves, tracheae, and genitalia. – Australian Journal of Zoology **15**: 961–998.

BLANKE A., GREVE C., WIPFLER B., BEUTEL R.G., HOLLAND B., MISOF B. 2013. The identification of concerted convergence in insect heads corroborates Palaeoptera. – Systematic Biology **62**: 250–263.

BLANKE A., KOCH M., WIPFLER B., WILDE F., MISOF B. 2014. Head morphology of *Tricholepidion gertschi* indicates monophyletic Zygentoma. – Frontiers in Zoology **11**: 16.

BLANKE A., WIPFLER B., LETSCH H., KOCH H., BECKMANN F., BEUTEL R., MISOF B. 2012. Revival of Palaeoptera - head characters support a monophyletic origin of Odonata and Ephemeroptera (Insecta). – Cladistics **28**: 560–581.

BRADLER S. 2009. Die Phylogenie der Stab- und Gespenstschrecken (Insecta: Phasmatodea). – Species, Phylogeny and Evolution **2**: 3–139.

BRESSLER K., SHELTON C. 1993. Ear foreign-body removal: A review of 98 consecutive cases. – The Laryngoscope **103**: 367–370.

BUDER G., KLASS K.-D. 2013. A comparative study of the hypopharynx in Dictyoptera (Insecta). – Zoologischer Anzeiger **252**: 383–403.

CHISHOLM P.J. 1962. The anatomy in relation to the feeding habits of *Perla cephalotes* Curtis (Plecoptera, Perlidae) and other Plecoptera. – Transactions of the Society for British Entomology **15**: 56–101.

COLGAN D.J., CASSIS G., BEACHAM E. 2003. Setting the molecular phylogenetic framework for the Dermaptera. – Insect Systematics & Evolution **34**: 65–79.

DJERNÆS M., KLASS K.-D., EGGLETON P. 2015. Identifying possible sister groups of Cryptocercidae + Isoptera: a combined molecular and morphological phylogeny of Dictyoptera. – Molecular Phylogenetics and Evolution **84**: 284–303.

DJERNÆS M., KLASS K.-D., PICKER M.D., DAMGAARD J. 2012. Phylogeny of cockroaches (Insecta, Dictyoptera, Blattodea), with placement of aberrant taxa and exploration of out-group sampling. – Systematic Entomology **37**: 65–83.

DORSEY G.K. 1943. The musculature of the labrum, labium and pharyngeal region of adult and immature Coleoptera. – Smithsonian Miscellaneous Collections **103**: 1–40.

DRILLING K., KLASS K.-D. 2010. Surface structures of the antenna of Mantophasmatodea (Insecta). – Zoologischer Anzeiger - A Journal of Comparative Zoology **249**: 121–137.

FRIEDEMANN K., WIPFLER B., BRADLER S., BEUTEL R.G. 2012. On the head morphology of *Phyllium* and the phylogenetic relationships of Phasmatodea (Insecta). – Acta Zoologica **93**: 184–199.

GEWECKE M. 1972. Bewegungsmechanismus und Gelenkrezeptoren der Antennen von *Locusta migratoria* L.(Insecta, Orthoptera). – Zeitschrift für Morphologie der Tiere **71**: 128–149.

GILES E.T. 1961. Further studies on the growth stages of *Arixenia esau* Jordan and *Arixenia jacobsoni* Burr (Dermaptera: Arixeniidae), with a note on the first instar antennae of *Hemimerus talpoides* Walker (Dermaptera: Hemimeridae). – Proceedings of the Royal Entomological Society of London. Series A, General Entomology **36**: 21–26.

GILES E.T. 1962. The comparative external morphology and affinities of the Dermaptera. – Transactions of the Royal Entomological Society of London **115**: 95–164.

GRIMALDI D.A., ENGEL M.S. 2005. Evolution of the Insects. – Cambridge University Press, Cambridge.

HAAS F. 2005. 12. Ordnung Dermaptera, Ohrwürmer. Pp. 172–180 in DATHE H.H. (ed.), Lehrbuch der Speziellen Zoologie, Band 1: Wirbellose, 5. Teil: Insecta. – Spektrum Akademischer Verlag, Heidelberg.

HAAS F., KUKALOVÁ-PECK J. 2001. Dermaptera hindwing structure and folding: New evidence for familial, ordinal and superordinal relationships within Neoptera (Insecta). – European Journal of Entomology **98**: 445–509.

HANSEN H.J. 1894. On the structure and habits of *Hemimerus talpoides* Walk. – Entomologisk Tidskrift **15**: 65–93.

HENNIG W. 1969. Die Stammesgeschichte der Insekten. – Kramer, Frankfurt (Main).

HENSON H. 1950. On the head capsule and mouthparts of *Forficula auricularia* Linn. (Dermaptera). – Proceedings of the Royal Entomological Society of London. Series A, General Entomology **25**: 10–18.

HOKE G. 1924. The anatomy of the head and mouth-parts of Plecoptera. – Journal of Morphology **38**: 347–385.

ISHIWATA K., SASAKI G., OGAWA J., MIYATA T., SU Z.-H. 2011. Phylogenetic relationships among insect orders based on three nuclear protein-coding gene sequences. – Molecular Phylogenetics and Evolution **58**: 169–180.

JARVIS K.J., HAAS F., WHITING M.F. 2005. Phylogeny of earwigs (Insecta: Dermaptera) based on molecular and morphological evidence: reconsidering the classification of Dermaptera. – Systematic Entomology **30**: 442–453.

JORDAN K. 1909. Notes on the anatomy of *Hemimerus talpoides*. – Novitates Zoologicae **16**: 327–330.

KADAM K. 1961. Studies on the morphology of an Indian earwig, *Labidura riparia*, Pall., var. *ineris*, Brunner. – Journal of the Zoological Society of India **13**: 34–49.

KAMP J.W. 1973. Numerical classification of the orthopteroids, with special reference to the Grylloblattodea. – Canadian Entomologist **105**: 1235–1249.

KHANDEKAR C.D. 1972. Nervous system of *Labidura riparia* (Dermaptera). – Deutsche Entomologische Zeitschrift **19**: 357–365.

KHANDEKAR C.D. 1973. Morphology of the stomodeal nervous system of *Labidura riparia* Pallas (Dermaptera, Labiduridae). – Deutsche Entomologische Zeitschrift **20**: 315–320.

KJER K.M. 2004. Aligned 18S and insect phylogeny. – Systematic Biology **53**: 506–514.

KJER K.M., CARLE F.L., LITMAN J., WARE J. 2006. A molecular phylogeny of Hexapoda. – Arthropod Systematics & Phylogeny **64**: 35–44.

KLAUSNITZER B., SCHIEMENZ H. 2010. Dermaptera – Ohrwürmer. Pp. 111–112 in KLAUSNITZER B (ed.), Exkursionsfauna von Deutschlands. Band 2. Wirbellose: Insekten. – Spektrum Akademischer Verlag, Heidelberg.

KOCAREK P., JOHN V., HULVA P. 2013. When the body hides the ancestry: phylogeny of morphologically modified epizoic earwigs based on molecular evidence. – PloS one **8**: e66900.

KÔMOTO N., YUKUHIRO K., TOMITA S. 2012. Novel gene rearrangements in the mitochondrial genome of a webspinner, *Aposthonia japonica* (Insecta: Embioptera). – Genome **55**: 222–233.

KÜHNLE K.F. 1913. Vergleichende Untersuchungen über das Gehirn, die Kopfnerven und die Kopfdrüsen des gemeinen Ohrwurms *Forficula auricularia*. – Jenaische Zeitschrift für Naturwissenschaften **50**: 147–276.

LETSCH H., SIMON S. 2013. Insect phylogenomics: new insights on the relationships of lower neopteran orders (Polyneoptera). – Systematic Entomology **38**: 783–793.

MA C., WANG Y., WU C., KANG L., LIU C. 2014. The compact mitochondrial genome of *Zorotypus medoensis* provides insights into phylogenetic position of Zoraptera. – BMW Genomics **15**: 1156.

MATSUMURA J., WIPFLER B., POHL H., DALLAI R., MACHIDA R., MASHIMO Y., CAMERA J.T., RAFAEL J.A., BEUTEL R.G. 2015. Cephalic anatomy of *Zorotypus weidneri* New, 1978: new evidence for a placement of Zoraptera in Polyneoptera – Arthropod Systematics & Phylogeny **73**: 85–105.

MISOF B., LIU S., MEUSEMANN K., PETERS R.S., DONATH A., MAYER C., FRANDSEN P.B., WARE J., FLOURI T., BEUTEL R.G., NIEHUIS O., PETERSEN M., IZQUIERDO-CARRASCO F., WAPPLER T., RUST J., ABERER A.J., ASPÖCK U., ASPÖCK H., BARTEL D., BLANKE A., BERGER S., BÖHM A., BUCKLEY T.R., CALCOTT B., CHEN J., FRIEDRICH F., FUKUI M., FUJITA M., GREVE C., GROBE P., GU S., HUANG Y., JERMIIN L.S., KAWAHARA A.Y., KROGMANN L., KUBIAK M., LANFEAR R., LETSCH H., LI Y., LI Z., LI J., LU H., MACHIDA R., MASHIMO Y., KAPLI P., MCKENNA D.D., MENG G., NAKAGAKI Y., NAVARRETE-HEREDIA J.L., OTT M., OU Y., PASS G., PODSIADLOWSKI L., POHL H., REUMONT VON B.M., SCHÜTTE K., SEKIYA K., SHIMIZU S., SLIPINSKI A., STAMATAKIS A., SONG W., SU X., SZUCSICH N.U., TAN M., TAN X., TANG M., TANG J., TIMELTHALER G., TOMIZUKA S., TRAUTWEIN M., TONG X., UCHIFUNE T., WALZL M.G., WIEGMANN B.M., WILBRANDT J., WIPFLER B., WONG T.K.F., WU Q., WU G., XIE Y., YANG S., YANG Q., YEATES D.K., YOSHIZAWA K., ZHANG Q., ZHANG R., ZHANG W., ZHANG Y., ZHAO J., ZHOU C., ZHOU L., ZIESMANN T., ZOU S., LI Y., XU X., ZHANG Y., YANG H., WANG J., WANG J., KJER K.M., ZHOU X. 2014. Phylogenomics resolves the timing and pattern of insect evolution. – Science **346**: 763–767.

MISOF B., NIEHUIS O., BISCHOFF I., RICKERT A., ERPENBECK D., STANICZEK A. 2007. Towards an 18S phylogeny of hexapods: Accounting for group-specific character covariance in optimized mixed nucleotide/doublet models. – Zoology **110**: 409–429.

Moulins M. 1968. Contribution a la connaissance anatomique des Plecoptères: la région céphalique de la larve de *Nemoura cinerea* [Nemouridae]. – Annales de la Societe Entomologique de France (NS) **4**: 91–143.

Moulins M. 1969. Étude anatomique de l'hypopharynx de *Forficula auricularia* L. (Insecte, Dermaptère): Téguments, musculature, organes sensoriels et innervations. Interprétation morphologique. – Zoologische Jahrbücher, Abteilung für Anatomie und Ontogenie der Tiere **86**: 1–27.

Naegle M.A., Mugleston J.D., Bybee S.M., Whiting M.F. 2016. Reassessing the phylogenetic position of the epizoic earwigs (Insecta: Dermaptera). – Molecular Phylogenetics and Evolution **100**: 382–390.

Nel A., Aria C., Garrouste R., Waller A. 2012. Evolution and palaeosynecology of the Mesozoic earwigs (Insecta: Dermaptera). – Cretaceous Research **33**: 189–195.

Pass G. 1988. Functional morphology and evolutionary aspects of unusual antennal circulatory organs in *Labidura riparia* Pallas (Labiduridae), *Forficula auricularia* L. and *Chelidurella acanthopygia* Gene (Forficulidae) (Insecta: Dermaptera). – International Journal of Insect Morphology and Embryology **17**: 103–112.

Pass G. 1991. Antennal circulatory organs in Onychophora, Myriapoda and Hexapoda: functional morphology and evolutionary implications. – Zoomorphology **110**: 145–164.

Pass G., Gereben-Krenn B.A., Merl M., Plant J., Szucsisch N., Tögel M. 2006. Phylogenetic relationships of the orders of Hexapoda: contributions from the circulatory organs for a morphological data matrix. – Arthropod Systematics & Phylogeny **64**: 165–203.

Pohl H. 2010. A scanning electron microscopy specimen holder for viewing different angles of a single specimen. – Microscopy Research and Technique **73**: 1073–1076.

Popham E.J. 1959. The anatomy in relation to feeding habits of *Forficula auricularia* L. and other Dermaptera. – Proceedings of the Zoological Society of London **133**: 251–300.

Popham E.J. 1985. The mutual affinities of the major earwig taxa (Insecta, Dermaptera). – Zeitschrift für Zoologische Systematik und Evolutionsforschung **23**: 199–214.

Rähle W. 1970. Untersuchungen an Kopf und Prothorax von *Embia ramburi* Rimsky-Korsakow 1906 (Embioptera, Embiidae). – Zoologische Jahrbücher, Abteilung für Anatomie und Ontogenie der Tiere **87**: 248–330.

Ross E.S. 1970. Biosystematics of the Embioptera. – Entomology **15**: 157–172.

Ryan C., Ghosh A., Wilson-Boyd B., Smit D., O'Leary S. 2006. Presentation and management of aural foreign bodies in two Australian emergency departments. – Emergency Medicine Australasia **18**: 372–378.

Sasaki G., Ishiwata K., Machida R., Miyata T., Su Z.H. 2013. Molecular phylogenetic analyses support the monophyly of Hexapoda and suggest the paraphyly of Entognatha. – BMC Evolutionary Biology **13**: 236.

Simon S., Schierwater B., Hadrys H. 2010. On the value of elongation factor-1[alpha] for reconstructing pterygote insect phylogeny. – Molecular Phylogenetics and Evolution **54**: 651–656.

Simon S., Narechania A., DeSalle R., Hadrys H. 2012. Insect phylogenomics: Exploring the source of incongruence using new transcriptomic data. – Genome Biology and Evolution **4**(12):1295–1309.

Slifer E.H. 1967. Sense organs on the antennal flagella of earwigs (Dermaptera) with special reference to those of *Forficula auricularia*. – Journal of Morphology **122**: 63–79.

Song N., Li H., Song F., Cai W. 2016. Molecular phylogeny of Polyneoptera (Insecta) inferred from expanded mitogenomic data. – Scientific Reports **6**: 36175.

Strenger A. 1950. Funktionsstudie des Kopfes von *Forficula auricularia*. – Zoologische Jahrbücher, Abteilung für Anatomie und Ontogenie der Tiere **70**: 557–575.

Terry M.D., Whiting M.F. 2005. Mantophasmatodea and phylogeny of the lower neopterous insects. – Cladistics **21**: 240–257.

Tilgner E.H., Kiselyova T.G., McHugh J.V. 1999. A morphological study of *Timema cristinae* Vickery with implications for the phylogenetics of Phasmida. – Deutsche Entomologische Zeitschrift **46**: 149–162.

v. Kéler S. 1963. Entomologisches Wörterbuch mit besonderer Berücksichtigung der morphologischen Terminologie. – Akademie-Verlag: Berlin.

Vishnoi H.S. 1956. The structure, musculature and mechanism of the feeding apparatus of the various castes of the termite *Odontotermes obesus* (Rambur) Part I. Clypeo-labrum. – Journal of the Zoological Society of India **8**: 1–18.

Wagner D.L., Liebherr J.K. 1992. Flightlessness in insects. – Trends in Ecology & Evolution **7**: 216–220.

Walker E.M. 1931. On the anatomy of *Grylloblatta campodeiformis* Walker 1. Exoskeleton and musculature of the head. – Annals of the Entomological Society of America **24**: 519–536.

Walker E.M. 1933. On the anatomy of *Grylloblatta campodeiformis* Walker 2. Comparisons of head with those of other orthopteroid insects. – Annals of the Entomological Society of America **26**: 309–344.

Waller A., Caussanel C., Jamet C. 1996. Variation morphologique des pieces buccales chez quelques Dermaptères. – Bulletin de la Société Entomologique de France **101**: 523–533.

Wan X., Kim M.I., Kim M.J., Kim I. 2012. Complete mitochondrial genome of the free-living earwig, *Challia fletcheri* (Dermaptera: Pygidicranidae) and phylogeny of Polyneoptera. – PloS one **7**: e42056.

Wang Y., Engel M.S., Rafael J.A., Dang K., Wu H., Wang Y., Xie Q., Bu W. 2013. A unique box in 28S rRNA is shared by the enigmatic insect order Zoraptera and Dictyoptera. – PloS one **8**: e53679.

Wipfler B. 2012. Polyneopteran head morphology and its phylogenetic implications. – Unpubl. PhD thesis, Biologisch Pharmazeutische Fakultät, FSU Jena.

Wipfler B., Courtney G.W., Craig D.A., Beutel R.G. 2012a. First µ-CT based 3D reconstruction of a dipteran larva – the head morphology of *Protanyderus* (Tanyderidae) and its phylogenetic implications. – Journal of Morphology **273**: 968–980.

Wipfler B., Klug R., Ge S.-Q., Bai M., Göbbels J., Yang X.-K., Hörnschemeyer T. 2015. The thorax of Mantophasmatodea, the morphology of flightlessness, and the evolution of the neopteran insects. – Cladistics **31**: 50–70.

Wipfler B., Machida R., Müller B., Beutel R.G. 2011. On the head morphology of Grylloblattodea (Insecta) and the systematic position of the order, with a new nomenclature for the head muscles of Dicondylia. – Systematic Entomology **36**: 241–266.

Wipfler B., Pass G. 2014. Antennal heart morphology supports relationship of Zoraptera with polyneopteran insects. – Systematic Entomology **39**: 800–805.

Wipfler B., Weissing K., Klass K.-D., Weihmann T. 2016. The cephalic morphology of the American roach *Periplaneta americana* (Blattodea). – Arthropod Systematics & Phylogeny **74**: 267–297.

Wipfler B., Wieland F., DeCarlo F., Hörnschemeyer T. 2012b. Cephalic morphology of *Hymenopus coronatus* (Insecta: Mantodea) and its phylogenetic implications. – Arthropod Structure & Development **41**: 87–100.

Wu H.Y., Ji X.Y., Yu W.W., Du Y.Z. 2014. Complete mitochondrial genome of the stonefly *Cryptoperla stilifera* Sivec (Plecoptera: Peltoperlidae) and the phylogeny of polyneopteran insects. – Gene **537**: 177–183.

Yoshizawa K. 2011. Monophyletic Polyneoptera recovered by wing base structure. – Systematic Entomology **36**: 377–394.

Yoshizawa K., Johnson K.P. 2005. Aligned 18S for Zoraptera (Insecta): phylogenetic position and molecular evolution. – Molecular Phylogenetics and Evolution **37**: 572–580.

Yuasa H. 1920. The anatomy of the head and mouth-parts of Orthoptera and Euplexoptera. – Journal of Morphology **33**: 251–307.

YU-HAN Q., HAI-YAN W., XIAO-YU J., WEI-WEI Y., YU-ZHOU D. 2014. Mitochondrial genome of the stonefly *Kamimuria wangi* (Plecoptera: Perlidae) and phylogenetic position of Plecoptera based on mitogenomes. – PloS one **9**: e86328.

ZHANG Z.Q. 2011. Phylum Arthropoda von Siebold, 1848. In: ZHANG Z.-Q.(ed.), Animal Biodiversity: An outline of higher-level classification and survey of taxonomic richness. – Zootaxa **3148**: 99–103.

ZHOU C., TAN M., DU S., ZHANG R., MACHIDA R., ZHOU X. 2016. The mitochondrial genome of the winter stonefly *Apteroperla tikumana* (Plecoptera, Capniidae). – Mitochondrial DNA **27**: 3030–3032.